AD-A174 768 THEORETICAL PROBLEMS CONCERNING RAILGUN DESIGN(U) 1/1
BATTELLE COLUMBUS LABS RESEARCH TRIANGLE PARK NC
R L LIBOFF NOV 86 ARFSD-CR-86022 DAAG29-81-D-0100

UNCLASSIFIED F/G 9/6 NL

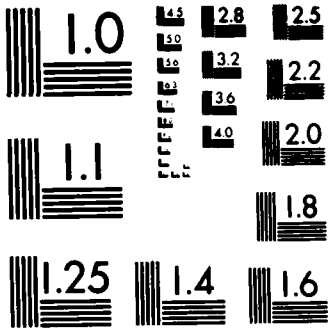

MICROCOPY RESOLUTION TEST CHART
NATIONAL BUREAU OF STANDARDS-1963-A

(2)

AD

~~AD-E401-595~~

AD-A174 768

CONTRACTOR REPORT ARFSD-CR-86022

THEORETICAL PROBLEMS CONCERNING RAILGUN DESIGN

RICHARD L. LIBOFF

BATTELLE COLUMBUS LABORATORIES
200 PARK DRIVE, P.O. BOX 12297
RESEARCH TRIANGLE PARK, NC 27709

GERALD L. FERRENTINO
PROJECT ENGINEER
ARDEC

DTIC
ELECTE
DEC 1 1986
S D
B

NOVEMBER 1986

US ARMY ARMAMENT MUNITIONS & CHEMICAL COMMAND
ARMAMENT RDE CENTER

U. S. ARMY ARMAMENT RESEARCH, DEVELOPMENT AND ENGINEERING CENTER

FIRE SUPPORT ARMAMENT CENTER

DOVER, NEW JERSEY

APPROVED FOR PUBLIC RELEASE; DISTRIBUTION IS UNLIMITED.

DTIC FILE COPY

86 12 01 000

UNCLASSIFIED

SECURITY CLASSIFICATION OF THIS PAGE (When Data Entered)

REPORT DOCUMENTATION PAGE

READ INSTRUCTIONS BEFORE COMPLETING FORM

1. REPORT NUMBER Contractor Report ARFSD-CR-86022	2. GOVT ACCESSION NO. AD-A174768
3. RECIPIENT'S CATALOG NUMBER	
4. TITLE (and Subtitle) Theoretical Problems Concerning Railgun Design	5. TYPE OF REPORT & PERIOD COVERED Final
	6. PERFORMING ORG. REPORT NUMBER
7. AUTHOR(s) Richard L. Liboff	8. CONTRACT OR GRANT NUMBER(s) DAAG29-81-D0100
9. PERFORMING ORGANIZATION NAME AND ADDRESS Battelle Columbus Laboratories 200 Park Drive, P.O. Box 12297 Research Triangle Park, NC 27709	10. PROGRAM ELEMENT, PROJECT, TASK AREA & WORK UNIT NUMBERS Delivery Order 1769
11. CONTROLLING OFFICE NAME AND ADDRESS ARDEC, IMD STINFO Div (SMCAR-MSI) Dover, NJ 07801-5001	12. REPORT DATE November 1986
	13. NUMBER OF PAGES 87
14. MONITORING AGENCY NAME & ADDRESS (if different from Controlling Office) U.S. Army Research Office P.O. Box 12211 Research Triangle Park, NC 27709	15. SECURITY CLASS. (of this report) Unclassified
	15a. DECLASSIFICATION/DOWNGRADING SCHEDULE

16. DISTRIBUTION STATEMENT (of this Report)

Approved for public release; distribution is unlimited.

17. DISTRIBUTION STATEMENT (of the abstract entered in Block 20, if different from Report)

18. SUPPLEMENTARY NOTES

This scientific services program task was requested and funded by the monitoring agency.

19. KEY WORDS (Continue on reverse side if necessary and identify by block number)

Railgun
One-component plasma
Equation of state
Strongly coupled plasma
Nonlinear electrical conductivity
Relativistic solution

20. ABSTRACT (Continue on reverse side if necessary and identify by block number)

Various theoretical studies associated with design and implementation of a railgun are presented. Among other items the report contains a new equation of state for a strongly coupled laboratory plasma as well as a new analytic expression for electrical conductivity for a strongly coupled plasma.

DD FORM 1 JAN 73 1473 EDITION OF 1 NOV 65 IS OBSOLETE

UNCLASSIFIED

SECURITY CLASSIFICATION OF THIS PAGE (When Data Entered)

CONTENTS

	Page
Introduction	1
Fundamental Relativistic Solution for a Railgun	3
Summary	3
Introduction	4
Analysis	5
Application	9
Conclusions	9
One-Component Plasma and Large Z Laboratory Plasma	15
Summary	15
Unified Equation of State for Weakly and Strongly Coupled Plasmas	23
Summary	23
Introduction	24
Analysis	26
Conclusions	31
Appendix A	33
Review of Electrical Conductivity in Plasmas	41
Summary	41
Introduction	42
Plasma Domains	42
Plasma Models	49
Historical Review	50
Electrical Conductivity	51
Conclusions	56
Nonlinear Electrical Conductivity for Strongly Coupled Plasmas	59
Summary	59
Introduction	61
Analysis	63
Conductivity	71
Evaluation of Conductivity	75
Conclusions	76
Appendix A	77
Appendix B	79
Appendix C	81
Appendix D	83
Distribution List	91

INTRODUCTION

This report addresses some theoretical problems associated with the railgun. It is comprised of five sections. In the first section a fully relativistic analysis is made of a simple prototype of the railgun. Electromagnetic field criteria are obtained for the realization of maximum propulsion speed. The second and third sections address an equation of state for a strongly coupled plasma. Results relevant to two-component plasma given in the second section are generalized to a multi-component plasma in the third section. A significant result of this work is exhibited in a plot of PV/Nk_BT vs. temperature T which exhibits variation with the shell structure of atoms in the plasma. Application is made specifically to an aluminum plasma.

Studies of electrical conductivity in a strongly coupled plasma are reviewed in the fourth section, and in the final section, an analytic expression is obtained for nonlinear electrical conductivity in strongly coupled plasmas. Figures and references as included at the end of each section.

DTIC
ELECTE
DEC 1 1986
S D
B

Accession For
NTIS
Dist
A-1

FUNDAMENTAL RELATIVISTIC SOLUTION FOR A RAIL GUN

Summary

A fully relativistic analysis is made of the dynamics of a rail-gun based on three assumptions: (1) Ohm's law is valid in the rest frame of the plasma; (2) total electron momentum is transferred to the projectile; and (3) motion of the projectile is constrained to one direction. With these assumptions, a relativistic equation for the velocity of the projectile is obtained whose solution monotonically increases to one of two values depending on field strengths. For B > E, the maximum velocity is cE/B whereas for E > B it is c where c is the speed of light, and E and B are applied electric and magnetic fields, respectively (in cgs).

INTRODUCTION

Attention has recently been given to dynamical properties of electromagnetic propulsion. In the rail-gun device,[1-5] a non-conducting projectile is propelled by a current-carrying plasma driven by the Lorentz force. Plasma dynamics is more difficult due to ablation of the projectile and for the most part previous studies have attempted to incorporate this effect.

In the present study, we return to a more elementary configuration for the purpose of developing a fully relativistic study of this problem. Thus, for example, it is assumed that the rest mass of the projectile is constant, and that total electron momentum from the plasma is transferred to the projectile. Furthermore, it is assumed that the projectile is constrained to move in one direction. Our remaining assumption is that Ohm's law is valid in the rest frame of the projectile.[6]

With these assumptions at hand, a relativistic equation is constructed for the projectile velocity. Solution to this equation reveals two asymptotic velocities which depends on initial field strengths. Thus, for example, for the case $E > B$, the velocity is c, the speed of light, whereas for $B > E$, the velocity is cE/B. It is further demonstrated that for initial velocities less than respective asymptotic values, velocities monotonically approach their respective limiting values. For the case $B > E$, starting velocities greater than cE/B are found to decay to this asymptotic value.

ANALYSIS

Our starting equation is Ohm's law, which in the rest frame of the projectile (primed coordinates) is written

$$\underset{\sim}{J}' = \sigma \underset{\sim}{E}' \tag{1}$$

where σ is conductivity. Transforming back to the lab frame (see Figure 1) we find

$$\begin{aligned} \gamma(J_x - c\,\beta\,\rho) &= \sigma E_x \\ J_y &= \sigma\,\gamma(E_y - \beta\,B_z) \\ J_z &= \sigma\,\gamma(E_z - \beta\,B_y) \end{aligned} \tag{2}$$

where $\beta \equiv v/c$ and $\gamma = (1-\beta^2)^{-1/2}$. The charge density ρ, for a charge-neutral plasma, is equal to zero. In the lab frame we take

$$\underset{\sim}{E} = E\hat{\underset{\sim}{y}} \tag{3}$$

$$\underset{\sim}{B} = B\hat{\underset{\sim}{z}}$$

where hatted variables denote unit vectors. Inserting these values into (2) gives

$$\underset{\sim}{J} = \sigma\,\gamma(E - \beta\,B)\hat{\underset{\sim}{y}} \tag{4}$$

with $\underset{\sim}{\xi}$ denoting microscopic electron velocity we write

$$\underset{\sim}{J} = qn\langle \underset{\sim}{\xi} \rangle \tag{5}$$

Electron charge and density are q and n respectively. We further recall that the density transforms as

$$n = \gamma n' \tag{6}$$

Combining the latter four equations gives

$$\langle \underset{\sim}{\xi} \rangle = \mu (E - \beta B) \hat{\underset{\sim}{y}} \tag{7}$$

where

$$\mu \equiv \frac{\sigma}{qn'} \tag{8}$$

represents mobility in the rest frame.

Taking the average of the Lorentz force on electrons we obtain

$$\frac{d}{dt} \langle p_y \rangle = \frac{q}{c} \langle \xi_y \rangle B \tag{9}$$

where we have recalled the vector property given by (7). We assume a total transfer of electron momentum to the projectile which gives

$$N \frac{d}{dt} \langle p_y \rangle \hat{\underset{\sim}{y}} = \frac{d}{dt} \underset{\sim}{P} \tag{10}$$

where N is total number of current-carrying electrons in the column. The momentum of the projectile, $\underset{\sim}{P}$, is given by

$$\underset{\sim}{P} = M \gamma \underset{\sim}{v} \tag{11}$$

where M is the mass of the projectile.

Combining (7), (9), (10), and (11) gives the desired equation of motion

$$\frac{d}{dt} \gamma M v = \frac{aI}{c} \left(1 - \frac{v}{w}\right) B \tag{12}$$

where a is the length of the conducting column, I is the current

$$aI = Nq\mu E \tag{13}$$

and

$$w \equiv \frac{cE}{B} \tag{14}$$

Note in particular that from (13) we may write

$$E = \frac{I}{A\sigma} \tag{15}$$

where aA represents the volume of the conducting column in the rest frame.

Integrating (12) gives

$$\eta - \eta_o = \frac{1}{c}\int_{v_o}^{v} \frac{du}{\left[1 - (\frac{u}{c})^2\right]^{3/2}(1 - \frac{u}{w})} \tag{15}$$

where η is the dimensionless time

$$\eta \equiv \frac{aIBt}{Mc^2} \tag{16}$$

and $v = v_o$ at $\eta = \eta_o$. From (15) we see that $\eta \to \infty$ at the singular paints $u = c$ and $u = w$ which represent asymptotic velocities. It will be shown below that these asymptotic velocities are approached monotonically. With this property we may conclude that for zero starting velocities maximum values are given by

$$E > B \qquad v_{max} = c \tag{17}$$

$$E < B \qquad v_{max} = w$$

A sketch of these findings is shown in Figure 2.

To examine the monotonicity of v(t) we differentiate (12) to obtain

$$\frac{1}{c}\frac{dv}{d\eta} = \left[1 - (\frac{v}{c})^2\right]^{3/2}\left[1 - \frac{v}{w}\right] \tag{18}$$

We conclude that for $v \leq c$ and $v \leq w$, $dv/d\eta \geq o$. Furthermore, with $v = o$ at $t = o$, (18) gives the starting acceleration (in dimensional form)

$$\left.\frac{dv}{dt}\right|_o = \frac{aIB}{Mc} \tag{19}$$

Note that for the case $E < B$, an initial velocity $v_o > w$, decays to $v = w$ as is evident from (18). Furthermore, as is clear from (15), asymptotic values (17) are independent of initial velocities.

Characteristic times corresponding to the maximum velocities (17) are as follows. In the limit $w >> c$, (12) gives the characteristic time

$$\tau_1 = \frac{Mc^2}{aIB} \tag{20}$$

with maximum velocity

$$v_{max}^{(1)} = c \tag{20a}$$

In the limit $w << c$, (12) has the solution (with $v = o$ at $t = o$),

$$v = w\left[1 - \exp(-t/\tau_2)\right] \tag{21}$$

where

$$\tau_2 = \frac{E}{B}\tau_1 \tag{22}$$

and

$$v_{max}^{(2)} = w \tag{22a}$$

We note that although $\tau_2 << \tau_1$, accelerations

$$\frac{v_{max}^{(1)}}{\tau_1} = \frac{v_{max}^{(2)}}{\tau_2}$$

are the same.

APPLICATION

In applying the preceding results to experimental values, first we rewrite w in practical units. Setting

$$E = \frac{V}{a} \tag{19}$$

where V is the potential across the rails, permits (14) to be rewritten

$$w = \frac{cV}{aB} \tag{20}$$

In practical units this expression becomes

$$w\left(\frac{km}{s}\right) = \frac{10^3 V(kV)}{B(kgauss)a(cm)} \tag{21}$$

Typical experimental values are[5,7]: V = 1kV, a ≃ 1cm, B ≃ 200 kgauss which gives w ≃ 5km/s. This value agrees in order-of-magnitude with observed maximum velocities.

CONCLUSIONS

We have examined the relativistic solution to the rail-gun configuration. Incorporating some simplifying assumptions we found that the projectile velocity goes monotonically to the minimum of the two velocities, c and cE/B. The asymptotic value c corresponds to E < B whereas the value cE/B corresponds to the limit B > E. It should be emphasized that this present study does not take into account thermodynamic effects such as momentum imparted to the projectile from the exploding "fuse."

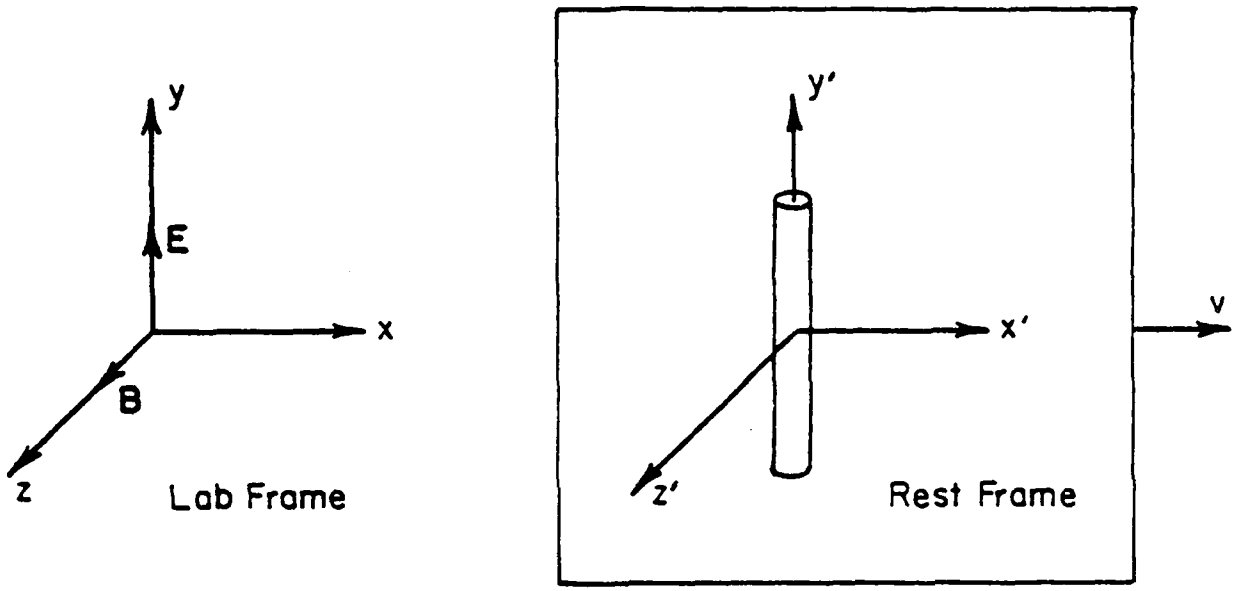

Figure 1. The lab frame and rest frame

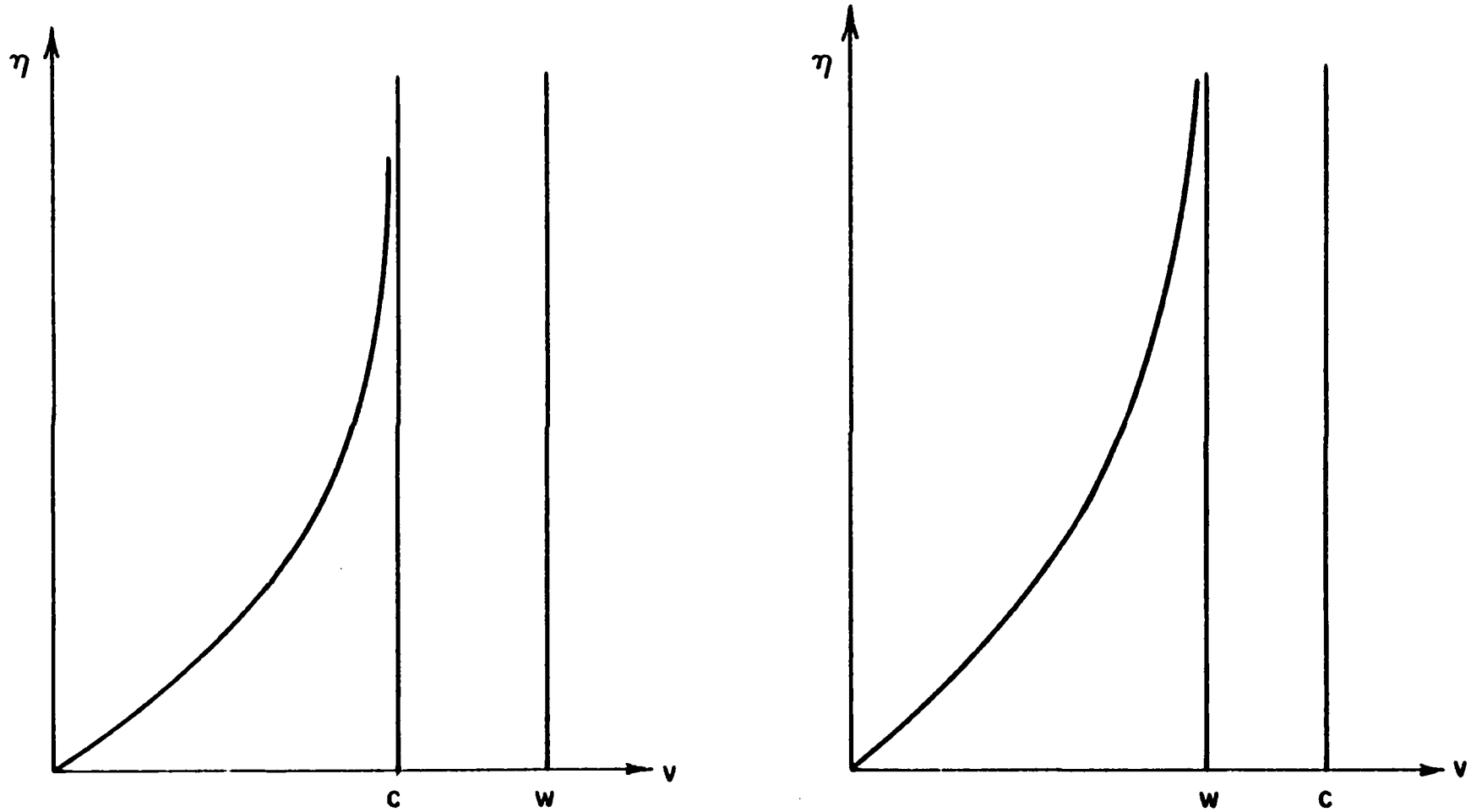

(a) E > B

The asymptotic speed c for E>B

(b) B > E

The asymptotic speed w for B>E

Figure 2. Dimensionless time as a function of projectile velocity v, with v=o at t=o

References

1. I.R. McNab, J.Appl.Phys. 51, 2549 (1980).

2. J.D. Powell and J.H. Batteh, J.Appl.Phys. 52, 2717 (1981).

3. J.D. Powell and J.H. Batteh, J.Appl.Phys. 54, 2242 (1983).

4. J.H. Batteh, J.Appl.Phys. 56, 3182 (1984).

5. A collection of papers on electromagnetic propulsion is given in IEEE Trans. on Magnetics, Mag-20, March (1984).

6. J.D. Jackson, Classical Electrodynamics, 2nd ed., John Wiley, New York (1975).

7. G. Ferrintino, personal communication.

ONE-COMPONENT PLASMA AND LARGE Z LABORATORY PLASMA

Summary

Stemming from an expression for the mean two-particle potential energy of a two-component laboratory plasma comprised of ions of charge Ze and electrons, it is argued that for sufficiently large Z, thermodynamic properties of such plasmas are the same as those relevant to Wigner's one-component plasma model. Thus the following equation of state is obtained for a laboratory plasma with $Z \gtrsim 5$ and $\Gamma \geq 1$.

$$\frac{P}{nk_BT} = 1 + \frac{d}{3} + \frac{1}{3}\left(\bar{a}\Gamma + b\Gamma^{1/4} + c\Gamma^{-1/4}\right)$$

In this equation, P is pressure, T is temperature, n is ion number density and $\bar{a}$, b, c, d are known numerical constants. The plasma parameter $\Gamma = (Ze)^2/ak_BT$ where $4\pi a^3/3$ represents mean occupation volume per ion.

Strongly-coupled plasmas play a role in recombination approaches to x-ray lasing [1], inertial-confinement fusion devices [2], the interiors of certain super-dense stars [3], and in plasma-driven rail-gun devices [4].

For the most part studies addressing strongly-coupled plasmas [5,6,7] have employed a plasma model due to Wigner [8] which was conceived for the purposes of studying phase transition to the solid state. This medium is called "jellium", or more commonly, a "one-component plasma", which often carries the abbreviation, OCP. An OCP is comprised of ions moving in a charge-neutralizing uniform negative background.

In the present work attention is directed at a laboratory plasma comprised of ions of charge Ze and electrons in equilibrium at a given temperature. Examining the interaction energy of the plasma indicates that for $Z \gtrsim 5$, thermodynamic properties such as internal energy and equation of state are given by corresponding expressions appropriate to an OCP. As an application of this finding, the equation of state for such a relatively high Z plasma is obtained from a previously constructed expression for the Helmholtz free energy [9].

With the plasma under consideration comprised of electrons and ions of charge eZ, charge neutrality implies the constraint

$$eV(n_e - Z\,n_Z) = 0 \tag{1}$$

where V is plasma volume and n_e and n_Z are electron and ion number densities, respectively. The approximate equality in

(1) derives from the inherent statistical nature of a plasma. For a two-component plasma, three interactions contribute to the mean two-particle potential energy and we write

$$\langle V\rangle \simeq (4\pi)^{1/3}[n_e^{1/3}e^2 - (n_e n_Z)^{1/6}Ze^2 + n_Z^{1/3}(Ze)^2] \qquad (2)$$

With the constraint (1) we may set $n_e = Z\,n_Z$ and (2) becomes

$$\langle V\rangle \simeq e^2(4\pi n_Z)^{1/3}(Z^{1/3} - Z^{7/6} + Z^2) \qquad (3)$$

Thus in the limit

$$Z^2 \gg Z^{1.17} \qquad (4)$$

the relation (3) reduces to

$$\langle V\rangle \simeq (4\pi n_Z)^{1/3}(Ze)^2 \qquad (5)$$

which we recognize to be the interaction potential of a one-component plasma comprised of ions of charge Ze.

This similarity may be further illustrated through the plasma parameter [10,11]

$$\gamma^{2/3} \simeq \frac{\langle V\rangle}{\langle E_K\rangle} \simeq \frac{\langle V\rangle}{k_B T} \qquad (6)$$

where $\langle E_K\rangle$ is mean kinetic energy per particle. The relevance of γ to the properties of a plasma is evident from (6). Namely, with this expression we may conclude that a plasma is strongly coupled when $\gamma \gtrsim 1$ and weakly coupled when $\gamma \ll 1$.

Substituting (5) into (6) gives (dropping the Z subscript on n_Z)

$$\gamma^{2/3} \simeq \frac{(Ze)^2(4\pi n)^{1/3}}{k_B T} \tag{7}$$

which, again, is the plasma parameter relevant to an OCP with ions of charge Ze.

The canonical expression for γ is given by

$$\gamma = \frac{1}{4\pi n \lambda_D^3} \tag{8}$$

where λ_D is the Debye distance.[13,14] With the latter two expressions we find

$$\lambda_D^2 = \frac{k_B T}{4\pi n (Ze)^2} \tag{9}$$

which is seen to be the Debye distance for an OCP comprised of ions of charge Ze.

These relations may be cast in terms of a plasma parameter more common to studies of OCP. It is given by

$$\Gamma = (Ze)^2/ak_B T \tag{10}$$

where a^3 is a measure of the mean occupation volume per ion. That is,

$$\frac{4}{3}\pi a^3 n = 1 \tag{11}$$

The parallel structure of γ and Γ is evidenced by rewriting (8):

$$\gamma = \frac{(Ze)^2/\lambda_D}{k_B T} \tag{12a}$$

$$\Gamma = \frac{(Ze)^2/a}{k_B T} \tag{12b}$$

so that

$$\gamma^2 = 3\,\Gamma^3$$

We may conclude that the previously stated criterion that separates weakly from strongly coupled plasmas may also be given in terms of Γ.

Thus we find that in the limit (4), the coupling and parameters of a two-component plasma of electrons and ions of charge Ze reduce to those relevant to an OCP of ions of charge Ze in a negative background. We may conclude that thermodynamic properties such as internal energy and equation of state for a two-component laboratory plasma with $Z \gg Z^{1.17}$ are the same as those of an OCP comprised of the same species of ions.

Numerical work of Slattery, Doolan and DeWitt [9] established the following expression for internal energy U for the fluid phase of an OCP.

$$\frac{U}{Nk_B T} = \bar{a}\Gamma + b\Gamma^{1/4} + c\Gamma^{-1/4} + d + \bar{e}\Gamma/N \tag{13}$$

where N is total ion number and

$$\bar{a} = -0.898, \quad b = 0.950, \quad c = 0.190,$$

$$d = -0.815, \quad \bar{e} = 0.010$$

The Helmholtz free energy, F, may then be obtained through integration. Namely,

$$\frac{F(\Gamma)}{Nk_BT} = \int_{\Gamma_1}^{\Gamma} \left[\frac{U(\Gamma')}{Nk_BT} + 3\right] d\Gamma' + \frac{F(\Gamma_1)}{Nk_BT} \tag{14}$$

The normalized free energy $F(\Gamma_1)/Nk_BT$, with $\Gamma_1 = 1$ was calculated employing various contributions over the unit interval. There results (in the limit of large N) [9]

$$\frac{F(\Gamma)}{Nk_BT} = \bar{a}\Gamma + 4(b\Gamma^{1/4} - c\Gamma^{-1/4}) + (d+3)\ln\Gamma - (\bar{a} + 4b - 4c + 1.152) \tag{15}$$

With this value of free energy at hand an equation of state is obtained from the thermodynamic relation

$$P = -\left(\frac{\partial F}{\partial V}\right)_T \tag{16}$$

To perform this differentiation we first rewrite Γ (10,12b) in explicit form

$$\Gamma = \frac{(Ze)^2}{k_BT}\left(\frac{4\pi N}{3V}\right)^{1/3} \tag{17}$$

There results

$$\frac{\partial\Gamma}{\partial V} = -\frac{\Gamma}{3V} \tag{18}$$

Differentiating (15) we obtain

$$\frac{1}{Nk_BT}\frac{\partial F}{\partial V} = [\bar{a} + b\Gamma^{-3/4} + c\Gamma^{-5/4} + (d+3)\Gamma^{-1}]\frac{\partial\Gamma}{\partial V} \tag{19}$$

With (16) and (18) we then obtain

$$\frac{PV}{Nk_BT} = 1 + \frac{d}{3} + \frac{1}{3}\left(\bar{a}\Gamma + b\Gamma^{1/4} + c\Gamma^{-1/4}\right) \tag{20}$$

With the previously stated argument we may conclude that (13) and (20) are valid energy and equation-of-state formulas for a laboratory plasma comprised of ions and electrons in equilibrium at a given temperature and obeying the constraint (4). Note in particular that for $Z = 5$ (completely ionized boron) $Z^{1.17}/Z^2 = 0.26$. For $Z = 13$ (completely ionized aluminum) this ratio becomes 0.12. Thus the proposed equivalence should be valid for $Z \gtrsim 5$. It is also important to note that this equivalence is not appropriate to processes where the dynamics of electrons come into play, such as conductivity [12].

References

1. D. M. Heffernan and R. L. Liboff, J. Plasma Phys. 27, 473 (1982).
2. K. Brueckner and S. Jorna, Revs. Mod. Phys. 46, 325 (1975).
3. E. E. Salpeter and H. M. Van Horn, Astrophys. J. 155, 183 (1969).
4. A collection of papers on electromagnetic propulsion is given in IEEE Trans. on Magnetics, Mag-20, March (1984).
5. S. Ichimaru, Revs. Mod. Phys. 54, 1017 (1982).
6. M. Baus and J. P. Hansen, Phys. Rep. 59, 1 (1980).
7. G. Kalman and P. Carini, Strongly Coupled Plasmas (Plenum, New York, 1978).
8. E. P. Wigner, Trans. Faraday Soc. (London) 34, 678 (1938).
9. W. L. Slattery, G. D. Doolen and H. E. Dewitt, Phys. Rev. A21, 2087 (1980); Phys. Rev. A26, 2255 (1982).
10. R. L. Liboff, J. Appl. Phys. 56, 2530 (1984)
11. P. M. Platzman and P. A. Wolf, Waves and Interactions in Solid State Plasmas (Academic, New York, 1973).
12. L. Spitzer, Jr., Physics of Fully Ionized Gases, (Interscience, New York, 1956).

UNIFIED EQUATION OF STATE FOR WEAKLY AND STRONGLY COUPLED PLASMAS

Summary

An argument is presented which permits a laboratory plasma of arbitrary ionization to be viewed as a one-component plasma. In this equivalence, effective ion charge number $\bar{Z}$ is dependent on temperature and ion number-density. The plasma parameter $\bar{\Gamma}$ thus gains additional dependence on these parameters due to its dependence on $\bar{Z}$. Employing previous results for the internal energy of such fluids gives the following unified equation of state for a laboratory plasma valid over the interval, $0 < \bar{\Gamma} < 300$.

$$PV = Nk_BT + \frac{1}{3}\left[U^*_{WC}(\bar{\Gamma})\Theta\left(\frac{1}{2} - \bar{\Gamma}\right) + U^*_{SC}(\bar{\Gamma})\Theta\left(\bar{\Gamma} - \frac{1}{2}\right)\right]$$

Here we have written U^*_{WC} and U^*_{SC}, respectively, for weakly and strongly-coupled excess energy and $\Theta(x)$ represents the unit step function. The volume, pressure, temperature, and number of ions in the plasma are written V, P, T and N, respectively. A numerical plot of this equation as a function of temperature reflects the shell structure of atoms in the plasma.

INTRODUCTION

The study of strongly-coupled plasmas is relevant to x-ray lasing,[1] inertial-confinement fusion devices,[2] the interior of certain super-dense stars,[3] and in plasma-driven rail-gun devices.[4] Studies of strongly-coupled plasmas have, for the most part,[5,6,7] utilized a model due to Wigner[8] in which the plasma is viewed as ions moving in a uniform charge-neutralizing background. This model is called a one-component plasma and carries the abbreviation OCP.

In an earlier work[9] a means of constructing the equation of state for a laboratory plasma was described which permitted use of OC results.[10] However the consistency of this analysis required a two-component fluid and therefore addressed fully ionized plasmas only.

In the present work, stemming from an analysis of Zel'dovich and Raizer,[11] the results of the aforementioned study are extended to a laboratory plasma of arbitrary ionization. The work of Zel'dovich-Raizer permits the plasma to be viewed as a two-component species comprised of electrons and ions with effective charge-number, $\bar{Z}$. The parameter $\bar{Z}$ emerges as an implicit function of temperature T and ion density, n. Thus the equation of state is found to contain additional temperature and density dependence in $\bar{Z}$ as it appears in the effective plasma parameter, $\bar{\Gamma}$.

The present work employs $\bar{\Gamma}$-dependent expressions for the internal energy previously obtained for strongly coupled[10] ($1 < \bar{\Gamma} < 300$) and weakly coupled[12] ($\bar{\Gamma} << 1$) OCP. The smooth connection of these two curves near $\bar{\Gamma} \approx 0.5$ motivates the extrapolation of the strongly-coupled form to the domain $0.5 \leq \bar{\Gamma} \leq 1$ This connecting segment results in a unified equation of state valid over the entire domain, $0 \leq \bar{\Gamma} < 300$.

Two interesting effects run through the analysis. The first of these pertains to the form of the effective plasma parameter

$$\bar{\Gamma} \propto \frac{n^{1/3}\,\bar{Z}^2\,(T,n)}{T}$$

For the most part, previous plasma studies did not view $\bar{Z}$ as temperature dependent. Under such circumstances, the plasma parameter grows large with decrease in temperature. However, in the present study $\bar{Z}$ is seen to increase monotonically with T (with steps at ionization shells) and we find an overall decrease of $\bar{\Gamma}$ with T. The second interesting observation is that the shell structure of atoms in the plasma is reflected in the equation of state.

As the analysis is dependent on the details of ionization energies, a specific material must be chosen prior to numerical work. The present study addresses aluminum.[13] Thus plots of PV/Nk_BT vs T as well as $\bar{\Gamma}$ (where P is pressure) are presented for n in the range 10^{15} - 10^{20} cm^{-3}. Plots are also included of $\bar{Z}$ vs T.

ANALYSIS

Review

Previous Finding

In ref. 9 it was noted that for a two-component plasma one may write the mean two-particle potential energy as

$$\langle V \rangle \approx \left(\frac{4\pi}{3}\right)^{1/3} \left[n_e^{1/3} e^2 - (n_e n)^{1/6} Ze^2 + n^{1/3} (Ze)^2 \right] \qquad (1)$$

where n_e and n are, respectively, electron and ion number density. With conservation of charge, $n_e = Zn$, (1) becomes

$$\langle V \rangle \approx \left(\frac{4\pi n}{3}\right)^{1/3} (Ze)^2 \qquad (2)$$

providing

$$Z^2 \gg Z^{1.17} \qquad (3)$$

We recognize (2) to be the average interaction potential of a OCP comprised of ions of charge Ze. A key parameter in the study of strongly-coupled plasmas is the plasma parameter, which with (2) is written

$$\Gamma \equiv \frac{\langle V \rangle}{k_B T} = \frac{\left(\frac{4\pi n}{3}\right)^{1/3} (Ze)^2}{k_B T} \qquad (4)$$

Thus a plasma is strongly coupled for $\Gamma \gtrsim 1$ and weakly coupled for $\Gamma \ll 1$.[14]

With these observations and employing a previously obtained expression for the internal energy of an OCP,[10] an equation of state was obtained relevant to the domain $1 \leq \Gamma < 300$.

Thermodynamic Relations

Prior to generalizing these results to a laboratory plasma of arbitrary ionization we present a brief review of basic thermodynamic relations relevant to a plasma.

An equation of state for a plasma is related to internal energy in the following manner (see Appendix A).

$$\frac{PV}{Nk_BT} = \frac{U^*}{3Nk_BT} + 1 \tag{5}$$

where we have set

$$U^* = U - \frac{3}{2} Nk_BT \tag{6}$$

Here U denotes total plasma energy and U^* "excess" internal energy. Note that if U^* is known, then with the thermodynamic relation

$$P = - \left.\frac{\partial F}{\partial V}\right|_T = - \frac{\partial F}{\partial \Gamma} \left.\frac{\partial \Gamma}{\partial V}\right|_T$$

and (4), we may write

$$\frac{PV}{Nk_BT} = \frac{\Gamma}{3} \frac{\partial}{\partial \Gamma} \left(\frac{F}{Nk_BT}\right)$$

where F is the Helmholtz free energy. Integrating the preceding equation at constant T gives, with (5),

$$\int_{\Gamma_o}^{\Gamma} \frac{d\Gamma}{\Gamma} \left(\frac{U^*}{Nk_BT} + 3\right) = \frac{F(\Gamma) - F(\Gamma_o)}{Nk_BT} \tag{7}$$

Thus knowledge of U^* as a function of Γ for a plasma gives both the equation of state (5) and the free energy (7).

Effective ionization

As noted in ref. 11, a plasma in Saha equilibrium at a given temperature is characterized by ions of effective charge $e\bar{Z}$, where e is (positive) electron charge. Thus, the results of ref. 9 carry over with Z replaced by an effective ion charge number, $\bar{Z}$. Specifically one may write (1) with Z replaced by $\bar{Z}$ and again we find reduction to (2) relevant to an OCP, in the domain (3).

The ion-charge number, $\bar{Z}(T,n)$ is obtained in the following manner. First the discrete ionization energies, I(Z), as a function of degree of ionization, Z, are connected by line segments, such as depicted in Fig. 1 for the case of aluminum.[13] This gives the continuous function $\bar{I}(\bar{Z})$. The function $\bar{Z}(T,n)$ is then obtained by solving the following implicit equation, which stems from the Saha equation as well as conservation of charge,

$$\bar{Z} = \frac{AT^{3/2}}{n} \exp - \frac{\bar{I}\left(\bar{Z} + \frac{1}{2}\right)}{T} \tag{8}$$

where $A = 6 \times 10^{21}\ \mathrm{cm}^{-3}\ \mathrm{eV}^{-3/2}$ and T is in eV. In the present work this procedure for obtaining $\bar{Z}(T,n)$ was carried out again for the case of aluminum. Results are shown in Fig. 2 for ion densities $(10^{15} - 10^{20})\ \mathrm{cm}^{-3}$.

The plasma parameter Γ, as given by (4), now includes additional temperature and density dependence through $\bar{Z}(T,n)$. That is,

$$\bar{\Gamma} = \frac{\left(\frac{4\pi n}{3}\right)^{1/3} [\bar{Z}(T,n)e]^2}{k_B T} \tag{9}$$

A plot of this parameter vs T is shown in Fig. 3.

Equation of State

Ordinarily for an OCP, $U^* = U^*(\Gamma)$. To incorporate our findings as described above in an equation of state we write $U^* = U^*(\bar{\Gamma})$, where $\bar{\Gamma}$ is given by (9) with $\bar{Z}$ determined from (8). Thus (5) becomes

$$\frac{PV}{Nk_B T} = \frac{U^*(\bar{\Gamma})}{3Nk_B T} + 1 \tag{10}$$

In the weakly coupled domain ($\Gamma \lesssim 0.5$), U^* was obtained[12] as a function of $\varepsilon = \sqrt{3}\,\Gamma^{3/2}$. Converting these results to a Γ-dependent function gives

$$\frac{U^*_{WC}(\Gamma)}{Nk_B T} = a_1\Gamma^{3/2} + b_1\Gamma^3 \ln\Gamma + c_1\Gamma^3 + d_1\Gamma^{9/2}\ln\Gamma + e_1\Gamma^{9/2} \tag{11a}$$

In the strongly-coupled domain,[9] over the interval $1 < \Gamma < 300$, we have

$$\frac{U^*_{SC}}{Nk_B T} = a_2\Gamma + b_2\Gamma^{1/4} + c_2\Gamma^{-1/4} + d_2 \tag{11b}$$

Constants have the following values

$$a_1 = -0.866 , \quad b_1 = -1.125 , \quad c_1 = -1.102$$

$$d_1 = -2.923 , \quad e_1 = 0.243$$

$$a_2 = -0.898 , \quad b_2 = 0.950 , \quad c_2 = 0.190 ,$$

$$d_2 = -0.815$$

Inserting these results into (10) gives two equations of state relevant, respectively, to the two said domains. Numerical plots (see Fig. 4) of these results strongly suggest an interpolation insert over the interval $0.5 < \Gamma < 1$, given namely by the strong coupling form (11).

With this interpretation at hand one is able to write a unified equation of state valid over the whole interval, $0 < \Gamma < 300$. Namely,

$$PV = Nk_BT + \frac{1}{3}\left[U^*_{WC}(\overline{\Gamma})\,\Theta\left(\frac{1}{2} - \overline{\Gamma}\right) + U^*_{SC}(\overline{\Gamma})\,\Theta\left(\overline{\Gamma} - \frac{1}{2}\right)\right] \tag{12}$$

where $\overline{\Gamma}$, U^*_{WC} and U^*_{SC} are given respectively, by (9) and (11), and $\Theta(x)$ is written for the unit step function $\Theta(x) = 1$, $x > 0$ and zero elsewhere.

In application of (12) one should recall that $\overline{\Gamma}$ is implicitly dependent on T and n through its dependence on $\overline{Z}$ given by (8). A numerical plot of PV/Nk_BT vs T obtained from (12) is shown in Fig. 5. Note that the shell structure of atoms in the plasma is reflected in this equation of state.

CONCLUSIONS

A unified equation of state was constructed for a laboratory plasma of arbitrary ionization. This was achieved by introducing an effective ion charge-number, $\bar{Z}(T,n)$, obtained from the equations of Saha equilibrium. This form of $\bar{Z}$ was then used to obtain a generalized plasma parameter, $\bar{\Gamma}(T,n)$. Employing this value of $\bar{\Gamma}$ in previously obtained expressions for internal energy, and effecting an interpolation over the internal $\frac{1}{2} < \bar{\Gamma} \leq 1$, gave a unified equation of state over the total interval $0 \leq \bar{\Gamma} < 300$ for effective ionization $\bar{Z}^2 >> \bar{Z}^{1.17}$. It is important to note that the equivalence between a laboratory and one-component plasma described in Section A.1 is not relevant to processes where the dynamics of electrons come into play, such as conductivity.[15]

Appendix A

In this appendix we wish to derive the relation (5) relevant to an OCP. First we recall the statistical mechanical relations[16]

$$\frac{U}{Nk_BT} = \frac{3}{2} + \frac{N}{2Vk_BT}\int_0^\infty u(r)g(r)4\pi r^2 dr \tag{A.1}$$

$$\frac{PV}{Nk_BT} = 1 - \frac{N}{6Vk_BT}\int_0^\infty u'(r)g(r)4\pi r^3 dr \tag{A.2}$$

In these expressions, $g(r)$ is the radial distribution function, and $u(r)$ is the two-particle interaction potential. Let us assume the form

$$u(r) \propto \alpha\, r^{-s} \tag{A.3}$$

where α and s are constants. Inserting the derivative

$$u'(r) = -\frac{su}{r}$$

into (A.2) gives

$$\frac{PV}{Nk_BT} = 1 + \frac{Ns}{6Vk_BT}\int_0^\infty u(r)g(r)4\pi r^2 dr \tag{A.4}$$

which may be combined with (A.1) to give

$$\frac{PV}{Nk_BT} = \frac{s}{3}\left(\frac{U}{Nk_BT} - \frac{3}{2}\right) + 1 \tag{A.5}$$

For the Coulomb interaction, $s = 1$, and (A.5) returns (5).

References

1. D. M. Heffernan and R. L. Liboff, J. Plasma Phys. 27, 473 (1982).

2. K. Brueckner and S. Jorna, Revs. Mod. Phys. 46, 325 (1975).

3. E. E. Salpeter and H. M. Van Horn, Astrophys. J. 155, 183 (1969).

4. A collection of papers on electromagnetic propulsion is given in IEEE Trans. on Magnetics, Mag-20, March (1984).

5. S. Ichimaru, Revs. Mod. Phys. 54, 1017 (1982).

6. M. Baus and J. P. Hansen, Phys. Rep. 59, 1 (1980).

7. G. Kalman and P. Carini, Strongly Coupled Plasmas (Plenum, New York, 1978).

8. E. P. Wigner, Trans. Faraday Soc. (London) 34, 678 (1938).

9. R. L. Liboff, "One-component plasma model large Z plasmas," Army Res. Office Rept. No. ARFSD-CR-86005, Feb., 1986.

10. W. L. Slattery, G. D. Doolen and H. E. Dewitt, Phys. Rev. A21, 2087 (1980); Phys. Rev. A26, 2255 (1982).

11. Ya. B. Zel'dovich and Yu. P. Raizer, Physics of Shock Waves and High-Temperature Hydrodynamic Phenomena, vol. 1 (Academic, New York, 1966).

12. E. G. D. Cohen and T. J. Murphy, Phys. Fluids 12, 1404 (1969).

13. CRC Hand. Chem. Phys. 65th ed. (CRC Press, Boca Raton, FL 1984).

14. R. L. Liboff, J. Appl. Phys. 56, 2530 (1984).

15. L. Spitzer, Jr., Physics of Fully Ionized Gases, (Interscience, New York, 1956).

16. D. A. McQuarrie, Statistical Mechanics (Harper and Row, New York, 1973).

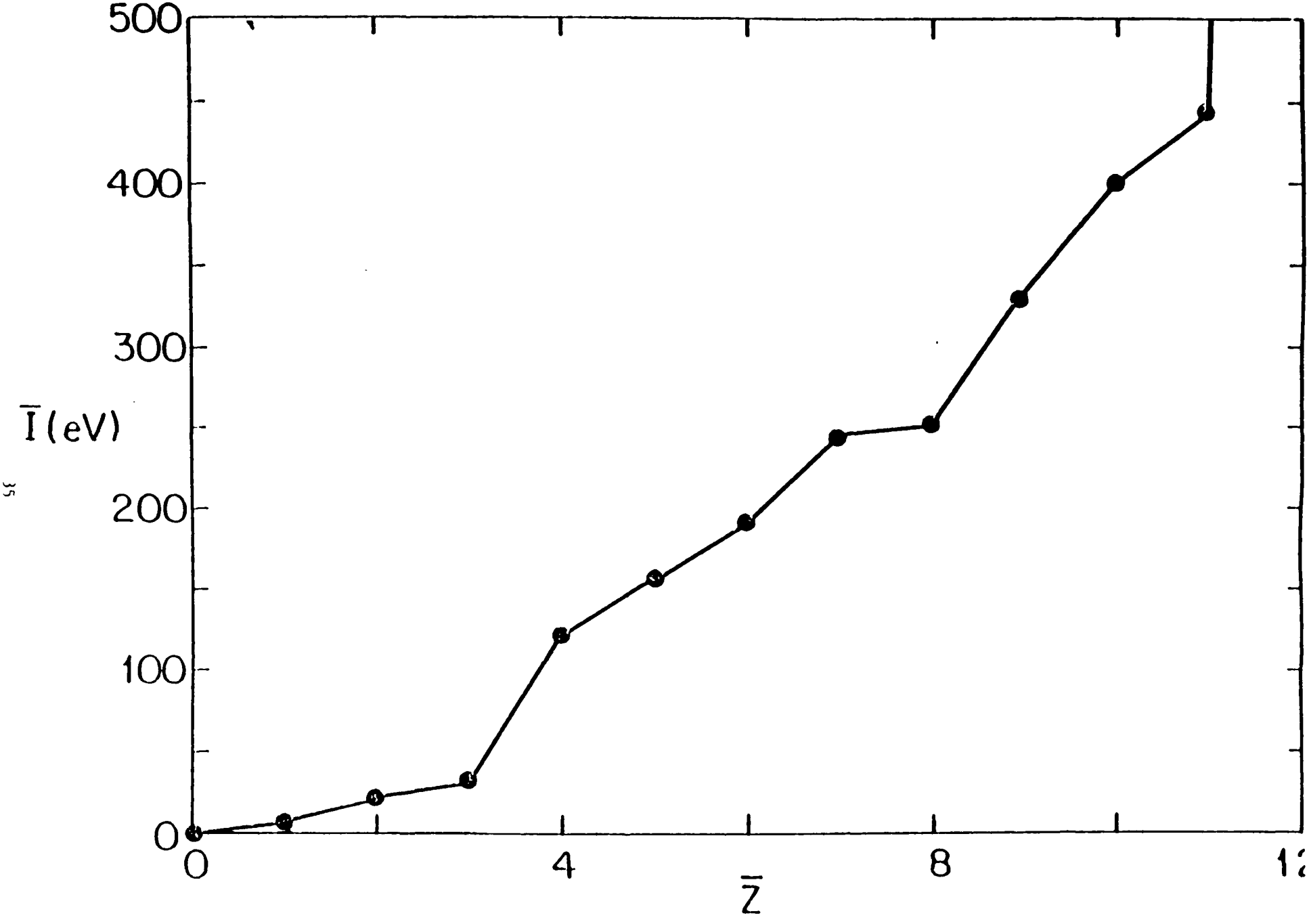

Figure 1. The continuous ionization energy curve, $\bar{I}=\bar{I}(\bar{Z})$ relevant to Al

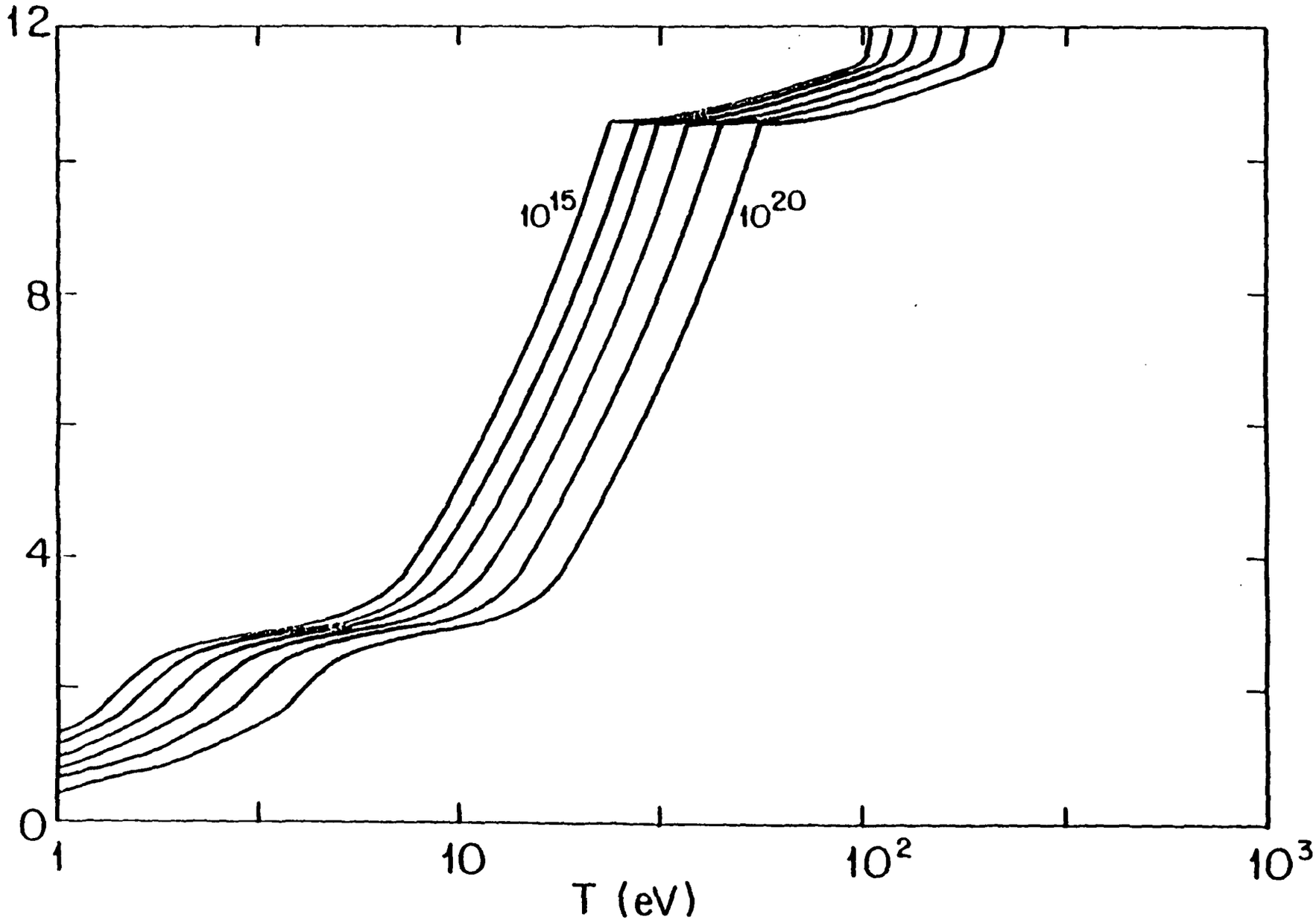

Figure 2. Average ionization $\bar{Z}$ vs. T(ev) at varying densities (cm^{-3})

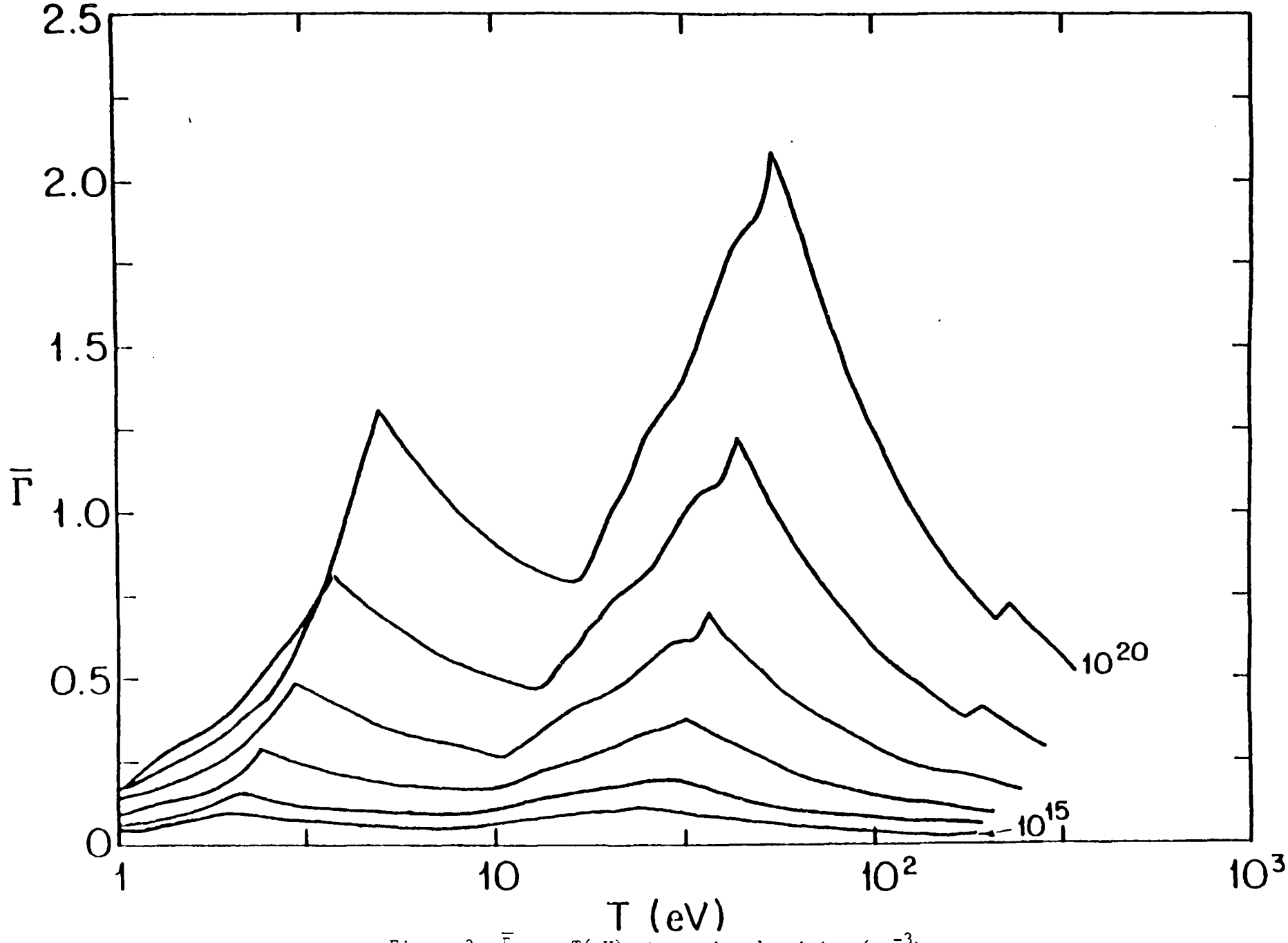

Figure 3. $\bar{\Gamma}$ vs. T(eV) at varying densities (cm^{-3})

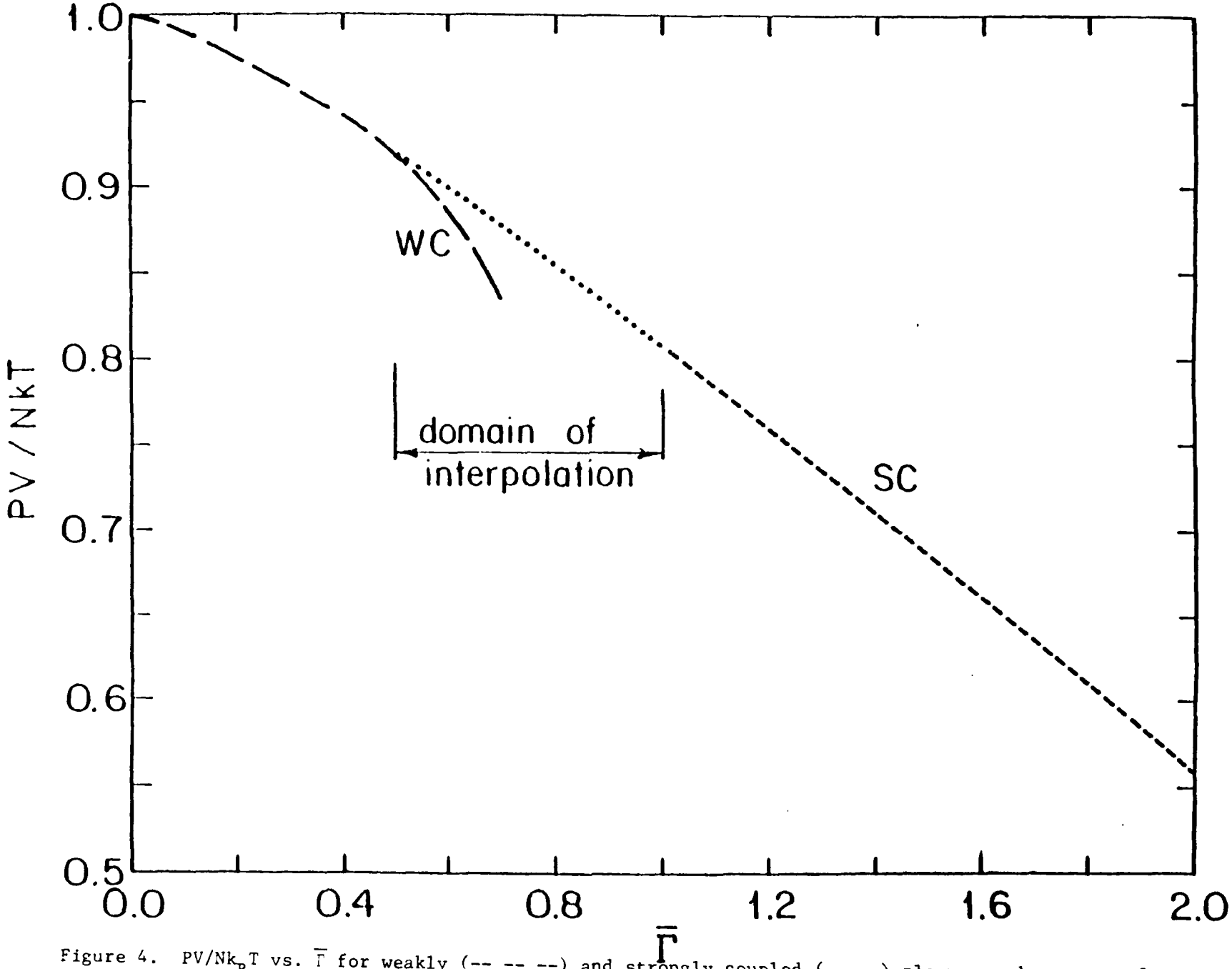

Figure 4. PV/Nk_BT vs. $\bar{\Gamma}$ for weakly (-- -- --) and strongly coupled (- - -) plasmas and segment of interpolation (. . .)

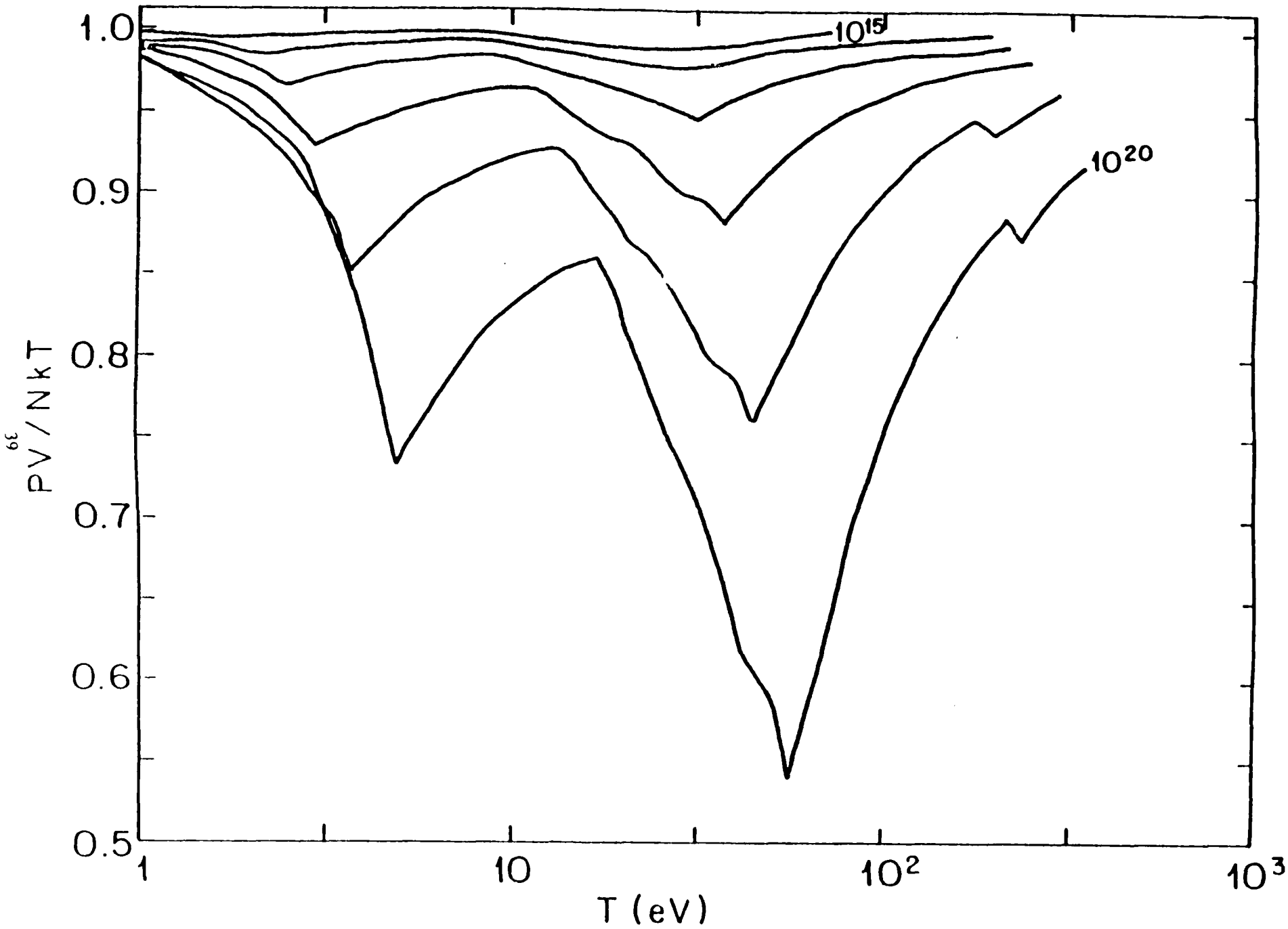

Figure 5. PV/Nk_BT vs. T at varying densities (cm^{-3})

REVIEW OF ELECTRICAL CONDUCTIVITY IN PLASMAS

Summary

A review of studies of electrical conductivity in a plasma is presented. A brief description of domains and parameters of plasma physics encountered in studies of conductivity is included. An historical account of conductivity calculations is given and it is concluded that one such study is most relevant to conductivity in a strongly-coupled classical plasma. Expressions and numerical results stemming from this study are included.

Introduction

The main thrust of this report addresses state-of-the-art studies of conductivity in a classical strongly-coupled plasma.

Preparatory to this discussion, in part II of the report, plasma domains are introduced and various important parameters are discussed relevant to the natural separation of these domains. A brief description of the fluid picture for a plasma is included as well as a discussion of domains relevant to the case where a magnetic field is present.

In part III various plasma models are introduced and a discussion of Saha equilibrium is included.

Part IV presents a brief historical review of electrical conductivity calculations for a plasma.

In part V formulas and results of numerical evaluation for electrical conductivity are presented. Values of electrical conductivity as a function of the plasma and compression parameters are given in a table at the conclusion of the report.

Plasma Domains

Parameters

Physical domains of a plasma divide into four basic areas[1] as depicted below.

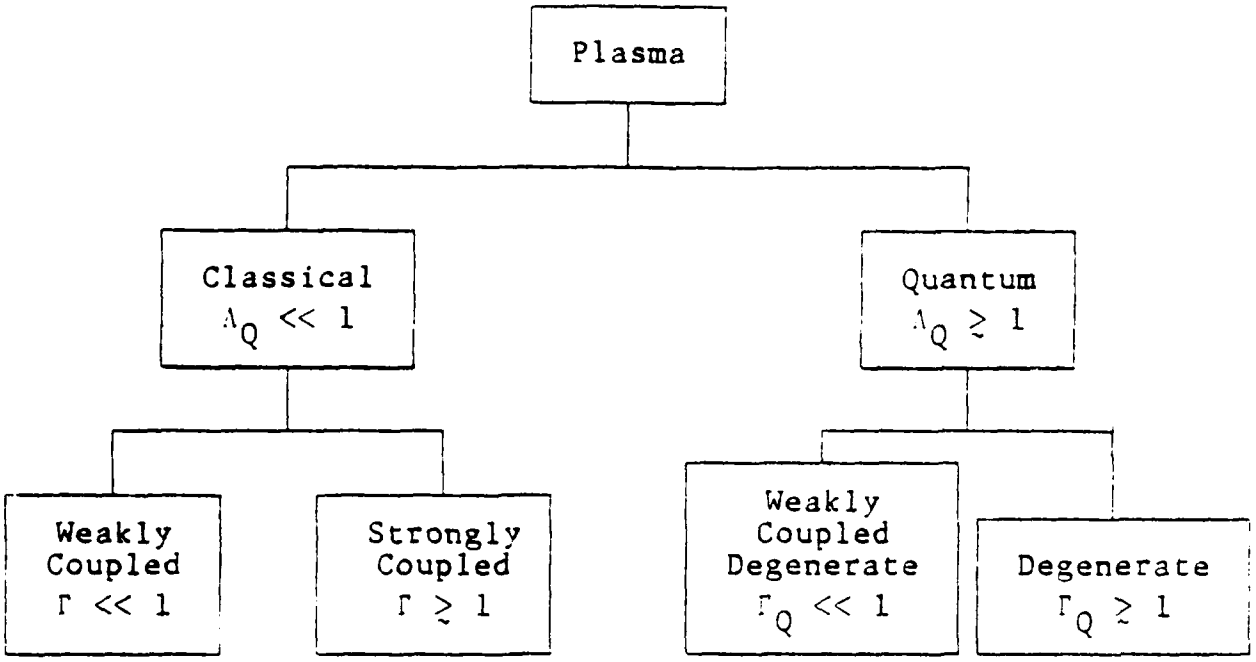

The parameters in the above inequalities are defined as follows. The quantum degeneracy parameter Λ is given by

$$\Lambda_Q = n \lambda_d^3 \tag{1}$$

where n is particle number density and

$$\lambda_d^2 = \frac{h^2}{2\pi m k_B T} \tag{2}$$

is the thermal deBroglie wavelength.

Thus, in the quantum domain $\lambda_d \gtrsim n^{-1/3}$, and the deBroglie wavelength is of the order of interparticle separation.

The plasma parameter

$$\Gamma = \frac{(Ze)^2}{ak_BT}$$

$$(4\pi a^3/3 = n_Z^{-1}) \tag{3}$$

is a measure of the ratio of mean two-particle ion potential to particle kinetic energy. Ion density is written n_Z. When $\Gamma << 1$, mean kinetic energy dominates potential interaction and the plasma is weakly coupled. In the limit $\Gamma \geq 1$ mean potential energy begins to dominate and the plasma is strongly coupled. For extreme potential dominance, $\Gamma >> 1$, and one expects the medium to undergo a phase change.[2,3]

The quantum parameter Γ_Q is defined as follows[1]

$$\Gamma_Q \equiv \frac{1}{6\pi n\lambda_{TF}^3} \tag{4}$$

where

$$\lambda_{TF}^2 \equiv \frac{\varepsilon E_F}{6\pi ne^2} \tag{5}$$

is the Thomas Fermi length,[4,5] E_F is the Fermi energy and ε is the dielectric constant of the medium. In the weakly coupled degenerate domain $\Gamma_Q << 1$ and densities grow so large that kinetic energy due to the uncertainty principle dominates potential energy.[6]

Fluid Picture

The plasma frequency is given by (in cgs)

$$\omega_p^2 = \frac{4\pi ne^2}{m} \tag{6}$$

Let ν denote the dominant collision frequency of plasma constituents. When

$$\nu \gg \omega_p \tag{7}$$

collisions tend to diminish collective plasma behavior and fluid behavior ensues.[7,8] This situation is depicted below.

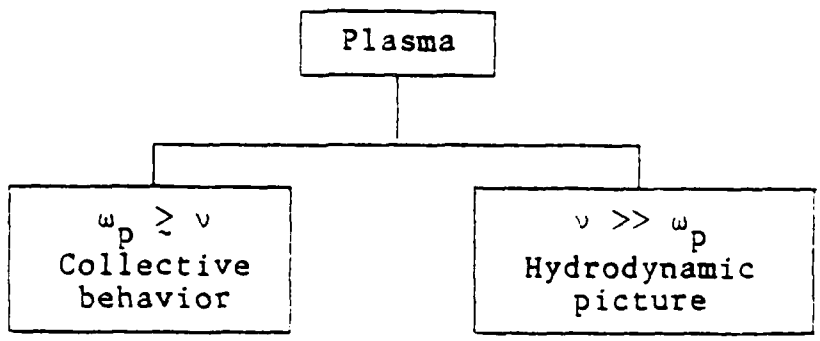

Magnetic Domains

If a magnetic field $\underset{\sim}{B}$ permeates the plasma then additional criteria come into play. We recall that a free particle of charge e and mass m undergoes circular motion in a magnetic field with frequency (cgs)

$$\Omega = \frac{eB}{mc} \tag{8}$$

If plasma particles suffer collisions at frequency ν, then at $\nu \gg \Omega$, the circular magnetic motion is lost to collisions and if further $\nu \gg \omega_p$ the plasma is fluid like.

If an electric field $\underset{\sim}{E}$ is also present then with Ohm's law (cgs)

$$\underset{\sim}{J} = \sigma\left(\underset{\sim}{E} + \frac{\underset{\sim}{J} \times \underset{\sim}{B}}{\rho c}\right) \tag{9}$$

where ρ is charge density and c is the speed of light. We may conclude that for $\rho E \gg JB/c$ the plasma is nonmagnetic. These criteria are listed below.

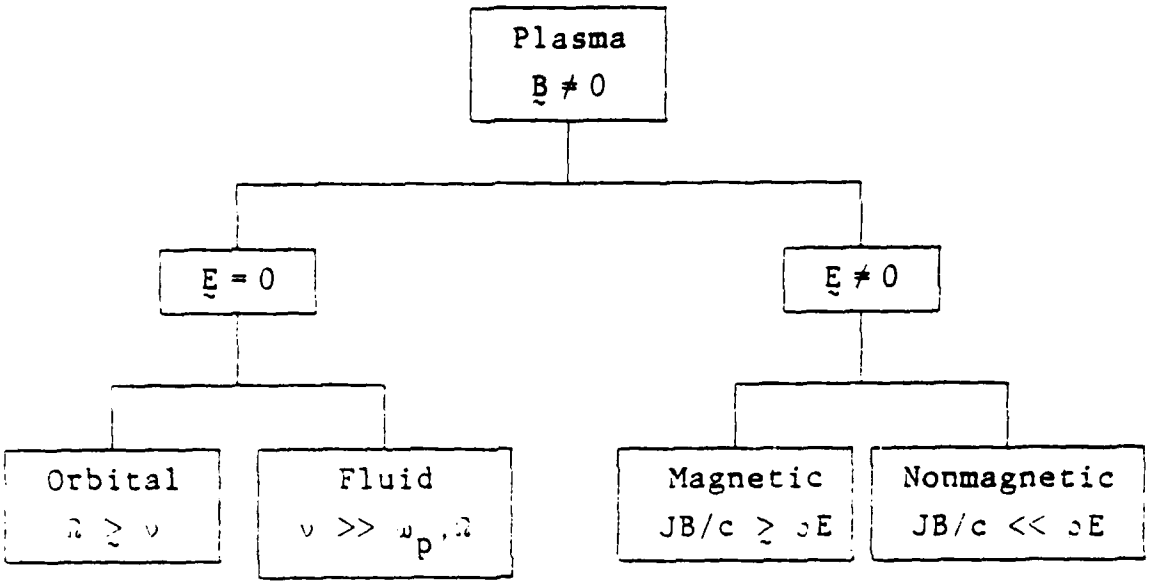

As previously noted, a plasma with a magnetic field is fluid-like for $\nu \gg \omega_p, \Omega$. If, further, $JB/c \gtrsim \rho E$, then we may term the plasma magnetofluid dynamic. Plasmas with $\nu \gtrsim \Omega$ are typically termed magnetohydrodynamic (MHD).[9]

An assortment of waves may propagate in a plasma in these various domains.[10,11,12]

Fluid Picture and Transport Coefficients

In concluding this section we estimate the conditions under which a plasma is fluid like with respect to specific transport processes. In making this estimate we recall that

different collision processes pertain to different transport coefficients. Thus, for example, in calculation of viscosity in a plasma, ion-ion collisions play the major role.[8] For this case we take the magnitude of the Coulomb ion-ion cross section to be

$$\sigma_{ii} \simeq \pi[(Ze)^2/k_BT]^2 = \pi\Gamma^2 a^2 \tag{10}$$

This gives the mean free path

$$\ell \simeq 1/n_Z\sigma_{ii} \tag{11}$$

and collision time

$$\tau \simeq \ell/\sqrt{k_BT/M} \tag{12}$$

where M and n_Z are mass and number density of the ion species. Combining these relations and recalling (3,6) we obtain (with $n = Zn_Z$)

$$\omega_p^2\tau^2 \simeq \frac{16}{3}\,\frac{M}{mZ}\,\frac{1}{\Gamma^3} \tag{13}$$

We may conclude that for calculation of viscosity, a fluid picture is appropriate for

$$\Gamma \gtrsim 21.4\,(A/Z)^{1/3} \tag{14}$$

where A is atomic mass.

For evaluation of electrical conductivity, electron-ion collisions dominate[8] and we write

$$\sigma_{ei} \simeq \frac{\pi Z^2e^4}{(k_BT)^2} \tag{15}$$

and

when atoms are stripped of all electrons leaving bare nuclei and electrons in the plasma.

Saha Equilibrium

The equilibrium state of a laboratory plasma is described by the Saha equation[15,16,17]

$$\frac{n_Z}{n_{Z-1}} = \frac{2u_Z}{u_{Z-1}} \frac{\exp(-\Delta E_Z/k_B T)}{n_e \lambda_d^3} \tag{19}$$

We have written n_Z for the density of ions of charge eZ and ΔE_Z is the ground state ionization energy for the transition $Z - 1 \rightarrow Z$. The electronic partition function u_Z is given by

$$u_Z = \sum_{i=0}^{i^*} g_Z^{(i)} \exp\left(\frac{-E_Z^{(i)}}{k_B T}\right) \tag{20}$$

where $g_Z^{(i)}$ and $E_Z^{(i)}$ are, respectively, statistical weight and excitation energy of the ith excited state of the Z ion. The series (20) terminates at the value i^* corresponding to orbits whose radii are comparable with mean distance between constituents of the plasma. It has been demonstrated by Zel'dovich and Raizer[17] that for a majority of ions, the ground-state term in (20) dominates over the remaining terms. Thus (20) reduces to

$$\frac{n_Z}{n_{Z-1}} = \frac{2g_Z^{(0)}}{g_{Z-1}^{(0)}} \frac{\exp(-\Delta E_Z/k_B T)}{n_e \lambda_d^3} \tag{21}$$

$$\ell \approx \frac{1}{n_Z \sigma_{ei}} \tag{16}$$

In this latter expression we have recalled that it is the 'target' ion density which is relevant. There results

$$\omega_p^2 \tau^2 \approx \frac{16}{3} \frac{M}{m} \frac{Z^3}{\Gamma^3} \tag{17}$$

Thus, for a fluid picture to be relevant for electrical conductivity one must have

$$\Gamma \gtrsim 21.4\, ZA^{1/3} \tag{18}$$

The inequalities (13) and (17) follow from the fluid-picture criterion (7).

Plasma Models

OCP and Other Models

A model often employed to describe a strongly coupled plasma is the so-called one-component plasma, which carries the abbreviation, OCP. This model is comprised of ions moving in a charge-neutral background. It was conceived by Wigner[13] to study phase change to the solid state. An extensive review of the physics of an OCP has been given by Ichimaru.[14] This model is often employed in the study of strongly coupled plasmas.

The simplest laboratory plasma model is that of a fully-ionized or two-component plasma comprised of electrons and ions of charge Ze. This situation is approached in the limit of very high temperature ($k_B T \gg I_Z$, I_Z = atomic ionization energy)

This equation indicates that in an actual laboratory plasma at finite temperature, all ionic species of atoms are present at varying relative densities.

Historical Review

Earliest expressions for electrical conductivity in a plasma are due to Spitzer and Härm[20] and Braginskii.[21] These results are relevant to a fully ionized nondegenerate weakly-coupled plasma.

These findings were improved upon by Rogers, DeWitt and Boercker[22] in a study of electrical conductivity in a partially ionized non-degenerate plasma. In this calculation the authors employed a Chapman-Enskog[23,24] expansion (with Sonine polynomials) of the Williams-DeWitt[25] kinetic equation. Scattering from electronic shells of ions and neutrals was treated using effective interaction potentials developed by Rogers.[26] We note that the Williams-DeWitt equation is the standard Boltzmann equation with quantum corrections entering through the scattering cross section. It is sometimes called a Balescu-Lenard equation due to shielding structure included in the interaction potential.

In the work of Boercker et al.[27] a plasma collision frequency is developed which correctly reduces to the Ziman[28,29] and Balescu-Lenard[25] results in appropriate limits. The Ziman formulation considers a strongly-coupled degenerate plasma at 0°K.

The work of ref. 27 is a generalization of Boercker's[30] in which a t-matrix formulation of the Kubo formula[31] is employed to calculate electrical conductivity.

Working with the Uehling-Uhlenbeck quantum generalized Boltzmann equation Lampe,[33] in an early study, employs a Chapman-Enskog expansion about the Fermi-Dirac distribution to calculate thermal conductivity, κ, which may be related to mobility, μ, through the Einstein relation

$$\mu = \frac{e\kappa}{nk_B T c_V}$$

Here we have written c_V for specific heat per particle in the plasma.

Lee and More[34] employ a Krook-Bhatnager-Gross[23] equation to calculate transport coefficients in a plasma. This technique depends on knowledge of the relaxation time which the authors calculate working with the Fermi-Dirac equilibrium distribution.

Electrical Conductivity

Strongly Coupled Classical Plasma

The most relevant expression for electrical conductivity in a strongly coupled quasiclassical plasma among those described in the preceding section, appears to be that obtained by Boercker et al.[27] It is given by

$$\sigma = \lambda(\Gamma)\ \frac{e^2 n}{m\nu} \tag{22}$$

where Γ, the plasma parameter, is given by (3). With $\beta \equiv (k_B T)^{-1}$, the collision frequency ν is given by

$$\nu = \frac{mn}{3Z}\left(\frac{\beta}{2\pi m}\right)^{3/2} \int_0^\infty \frac{dk\, k^3\, e^{-\beta\hbar^2 k^2/8m}\, u_{ei}(k) v_{ei}(k)}{\varepsilon(k,o)} \tag{23}$$

$$[S_{ee}(k)S_{ii}(k) - S_{ei}(k)S_{ie}(k)]$$

A closely allied expression for ν was obtained by Baus et al.[35] In (23), $S_{ab}(k)$ is the (dimensionless) dynamic structure factor relevant to the two components, a and b. The electron-ion Fourier transformed potential is $v_{ei}(k)$ and the Fourier transformed generalized potential is $u_{ei}(k)$. These potentials have dimensions of energy x volume. The transform $u_{ei}(k)$ satisfies the relation

$$u_{ab}(k) = -c_{ab}(k)/\beta$$

where $c_{ab}(k)$ is the Fourier transform of the direct correlation function.[36,37] The factor $\lambda(\Gamma)$ in (22) is a correction factor to account for the fact that ν as given by (23) is equivalent to a single-Sonine polynomial approximation.

A rough estimate of $\lambda(\Gamma)$ is obtained in the weak-coupling limit which gives

$$\lambda = \frac{1.93\, \omega_D\, (3\pi/2)^{1/2}}{4\pi\Gamma^{3/2}\Lambda} \tag{24}$$

$$\approx \frac{\omega_D}{2\Gamma^{3/2}\Lambda}$$

(Recall that in cgs units σ has the dimensions of frequency.) The function Λ is given by

$$\Lambda \equiv \frac{-1}{4\pi e^2} \int_0^\infty dk\, e^{-\beta\hbar^2 k^2/8m} k \frac{u_{ei}(k)}{|\varepsilon(k,o)|^2} S_{ii}(k) \tag{25}$$

In the Debye-Hückel limit one obtains

$$\begin{aligned} \Lambda &= e^{1/\alpha} E_1 (1/\alpha) - \frac{1}{2} e^{1/2\alpha} E_1 (1/2\alpha) \\ &\sim \frac{1}{2} (\ln \alpha - \gamma - \ln 2) \simeq \frac{1}{2} (\ln \alpha - 1.27) \end{aligned} \tag{26}$$

where

$$\alpha = \frac{8m}{\beta\hbar^2 k_D^2} ,$$

$E_1(x)$ is the exponential integral and γ is Euler's constant.

Numerical Results

Numerical evaluation of Λ given by (25) was performed using direct correlation functions and structure factors from solution of the hypernetted chain equation (HNC).[37] With these values of Λ inserted into (22,23), numerical integration for σ/ω_p was performed[27] at two values of the compression parameter[1,6,36]

$$r_s \equiv a/a_o$$

where a_o is the Bohr radius. Values of σ/ω_p stemming from the Debye-Hückel result (26) were also obtained. These values are listed in Table 1.

Table 1. Value of conductivity at varying Γ and r_s

Γ	r_s	$(\sigma/\omega_p)_{HNC}$		$(\sigma/\omega_p)_{DH}$	
0.05	0.4-	16.2		14.6	
	1.0		12.7		11.9
0.1	0.4-	8.61		7.69	
	1.0		6.16		5.77
0.2	0.4-	5.33		4.52	
	1.0		3.36		3.12
0.5	0.4-	4.13		3.55	
	1.0		2.07		1.87
1.0	0.4-	5.29		4.88	
	1.0		2.13		1.88
2.0	0.4-	12.3		11.6	
	1.0		3.72		3.11

Conclusions

A review of studies of electrical conductivity in a plasma has been presented. The report began with a description of domains and parameters of plasma physics common to such studies. An historical account of calculations led to the conclusion that the formulas most germain to conductivity in a classical strongly coupled plasma were those obtained by Boercker et al.[27] These findings were reported in section V concluding with a list of numerical results given in Table 1.

Acknowledgments

I am grateful to G. K. Schenter for his assistance in preparing this report and his careful reading of the final manuscript. This research was supported in part by a contract with Battelle Columbus Lab.

References

1. R. L. Liboff, J. Appl. Phys. 56, 2530 (1984); 58, 4438 (1985).

2. S. G. Brush, E. Teller, J. Chem. Phys. 45, 2102 (1966).

3. W. I. Slattery, G. D. Doolen and H. E. DeWitt, Phys. Rev. A 26, 2255 (1982).

4. N. F. Mott and H. Jones, Theory of Metals and Alloys (Dover, New York, 1958).

5. I. Ishihara, Statistical Physics (Academic, New York, 1971).

6. M. Gell-Mann and K. Brueckner, Phys. Rev. 106, 364 (1957).

7. B. Bernu and P. Vieillefosse, Phys. Rev. A 18, 2345 (1978).

8. L. Spitzer, Jr., Physics of Fully Ionized Gases, Interscience, New York, 1956).

9. D. R. Nicholson, Introduction to Plasma Theory, John Wiley (1983)

10. R. L. Liboff, Phys. Fluids 5, 963 (1962).

11. J. F. Denisse and J. L. Delcroix, Plasma Waves, Interscience, New York (1963).

12. J. G. Linhart, Plasma Physics, North-Holland, 2nd ed, New York (1961).

13. E. P. Wigner, Phys. Rev. 46, 1002 (1934); Trans. Faraday Svc. 34, 678 (1938).

14. S. Ichimaru, Revs. Mod. Phys. 54, 1017 (1982).

15. R. L. Liboff, E. J. Dorchak and B. Yaakobi, Acta. Phys. Slov. 29, 295 (1979).

16. W. B. Kunkel, ed. Plasma Physics in Theory and Applications (McGraw Hill, New York 1966).

17. D. M. Heffernan and R. L. Liboff, J. Plasma Phys. 27, 473 (1982).

18. B. M. Smirnov, Introduction to Plasma Physics, Mir, Moscow (1977).

19. Ya. B. Zel'dovich and Yu. P. Raizer, Physics of Shock Waves and High Temperature Hydrodynamic Phenomena, vol. 1, Academic, New York (1966).

20. L. Spitzer and R. Härm, Phys. Rev. 89, 977 (1953).

21. S. I. Braginskii, Sov. Phys. JETP, 6, 358 (1958).

22. F. J. Rogers, H. E. DeWitt and D. B. Boercker, Phys. Letts 82A, 331 (1981).

23. R. L. Liboff, Introduction to the Theory of Kinetic Equations, Krieger Publishing, Melbourne, FL (1979). Sonine polynomials were first used in a Chapman-Enskog expansion by Burnett, Proc. London Math. Soc. 39, 385 (1935).

24. S. Chapman and T. G. Cowling, The Mathematical Theory of Non-Uniform Gases, 3rd ed. Cambridge, London (1970).

25. R. H. Williams and H. E. DeWitt, Phys. Fluids 12, 2326 (1969).

26. F. J. Rogers, "Analytic Electron-Ion Effective Potentials for $Z \leq 55$, VCRL-84868 (1980).

27. D. B. Boercker, F. J. Rogers and H. E. DeWitt, Phys. Rev. A 25, 1623 (1982).

28. J. M. Ziman, Philos. Mag. 6, 1013 (1961).

29. H. Minoo, C. Deutsch and J. P. Hansen, Phys. Rev. A 14, 840 (1976).

30. D. B. Boercker, Phys. Rev. A 23, 1969 (1981).

31. R. Kubo, in Lectures in Theoretical Physics vol. I, W. E. Britten and L. G. Dunham ed. Interscience, New York (1959).

32. E. A. Uehling and G. E. Uhlenbeck, Phys. Rev. 43, 552 (1933).

33. M. Lampe, Phys. Rev. 170, 306 (1968).

34. Y. T. Lee and R. M. More, Phys. Fluids 27, 1273 (1984).

35. M. Baus, J. P. Hansen, and L. Sjogren, Phys. Lett 82A 180 (1981).

36. D. L. Goodstein, States of Matter, Prentice Hall, Englewood Cliffs, N. J. (1975).

37. F. J. Rogers, J. Chem. Phys. 73, 6272 (1980).

NONLINEAR ELECTRICAL CONDUCTIVITY FOR STRONGLY COUPLED PLASMAS

Summary

A nonlinear analysis of electrical conductivity in a plasma is given stemming from the Uehling-Uhlenbeck equation. Anisotropy due to an applied electric field is incorporated through a Legendre polynomial expansion of the distribution function. The plasma is comprised of ions, electrons and a neutral component. The electron-ion interaction is described by a shielded Debye potential at high energy and a cut-off Coulomb potential at low energy. A nonlinear equation for the distribution function is solved and yields

$$\bar{f}_{SL}(x) = \frac{1}{1 + Be^{A(x)}}$$

for the symmetric part of the solution. Nondimensional energy is x, B is a normalization constant and A(x) is an explicit integral dependent on the electric field and specifics of the interaction. Resulting nondimensional conductivity $\tilde{\sigma}$, is given by

$$\tilde{\sigma} = \frac{1}{3}\left(\frac{2}{\pi}\right)^{3/2} \frac{a_C(Z+1)^{1/2}}{\Lambda_Q \Gamma_D} \int_0^\infty \bar{f}_{SL}(x) \frac{d}{dx}\left(\frac{x}{\tilde{Q}}\right) dx$$

where Z is effective ionization, a_C is the ratio of charge to total heavy-particle density, $\tilde{Q}$ is dimensionless, weighted cross section and Λ_Q and Γ_D are quantum and plasma parameters respectively. Application is made to an aluminum plasma and plots of conductivity vs electric field are obtained. These plots exhibit three distinct regions. With increase in field strength these are: Ohmic, Coulomb-dominated and neutral-dominated.

Introduction

Previous kinetic studies of electrical conductivity in plasmas have, for the most part, involved linear theory. Thus, for example, approaches based on the Kubo[1,2] formula involve linear response theory; those based on a Chapman-Enskog expansion employ a linearized collision integral in the Boltzmann equation;[3,4] whereas others start with a linear equation[5] such as the linear Krook equation,[6] or the linearized Fokker-Planck equation.[7] As a consequence, such analyses can obtain expressions for current which, at best, are linearly dependent on electric field.

The present non-linear analysis begins with the Uehling-Uhlenbeck[8] quasi-classical kinetic equation. A Lorentz expansion[9] of the distribution function in terms of Legendre Polynomials[10,11,12] is employed to account for anisotropy in the distribution function due to the presence of an electric field. The analysis addresses a three-component plasma comprised of electrons, heavy ions of arbitrary ionization Z, and neutrals. These latter two components are assumed to be in equilibrium. The interaction between electrons and ions is described by a shielded Coulomb potential. It is found that the presence of the neutral component inhibits over population of the tail of the distribution function, better known as the 'runaway effect'.[13]

Two key parameters which enter the analysis are the Debye plasma parameter Γ_D and quantum degeneracy parameter, Λ_Q.[14] Thus when $\Gamma_D \gtrsim 1$ the plasma is termed strongly coupled and when $\Lambda_Q \gtrsim 1$ it is degenerate. The present work bridges the quasi-classical ($\Lambda_Q \approx 1$) and classical domains ($\Lambda_Q << 1$). Furthermore, apart from the assumption of a specific interaction potential, the analysis should prove valid in the strongly-coupled domain as well.

A nonlinear equation is obtained for the symmetric part of the distribution and solved exactly. In the limit of zero electric field the total distribution reduces to the Fermi Dirac distribution. For small-electric field it gives the displaced Fermi Dirac distribution. In the classical domain it returns the Druyvesteyn distribution.[10,15]

Integrating the total distribution function gives a closed expression for conductivity as a function of electric field. Numerical integration at constant heavy-particle temperature, density and ionization, yields conductivity vs electric field for various values of ion density. For reasonable charge densities three distinct regions are evident. At low field values Ohm's law is obeyed. At intermediate fields the conductivity rises due to effects of the Coulomb cross section. At high fields the hard core potential of the neutral component dominates yielding the familiar $E^{-1/2}$ fall off of conductivity.[16]

Analysis

Starting equation

Our starting equation is the Uehling-Uhlenbeck quasi-classical kinetic equation,[8] appropriate to a plasma comprised of electrons, ions and neutrals. It is assumed that ions and neutrals are of the same mass, M, and are both in equilibrium at the temperature T. These equilibrium distributions are given by

$$F_C(\underset{\sim}{v}_1) = a_C F_o(\underset{\sim}{v}_1)$$
$$F_N(\underset{\sim}{v}_1) = a_N F_o(\underset{\sim}{v}_1) \tag{1}$$

where

$$F_o(v_1) = n_o\left(\frac{M}{2\pi k_B T}\right)^{3/2} e^{-Mv_1^2/2k_BT} \tag{2}$$

and $a_C n_o$ and $a_N n_o$ are ion and neutral number densities respectively. With $a_N + a_C = 1$, n_o represents total heavy-particle number density.

With these assumptions our starting kinetic equation for the electron distribution function, $f(\underset{\sim}{x},\underset{\sim}{v},t)$ is given by

$$\frac{\partial f}{\partial t} + \underset{\sim}{v} \cdot \frac{\partial f}{\partial \underset{\sim}{x}} + \frac{e\underset{\sim}{E}}{m} \cdot \frac{\partial f}{\partial \underset{\sim}{v}} = \hat{J}_C(f,F_C) + \hat{J}_N(f,F_N) \tag{3}$$

where $\underset{\sim}{E}$ is applied electric field and m is electron mass. The collision integrals are given by (in Boltzmann notation[17])

$$J_i(f,F) = \int[f'(1-\xi f)F_1' - f(1-\xi f')F_1]\sigma_i g d\Omega d\underset{\sim}{v}_1 \tag{4a}$$

where

$$\xi \equiv (2\pi\hbar/m)^3, \qquad g = |\underset{\sim}{v} - \underset{\sim}{v}_1| \tag{4b}$$

and F denotes either F_C or F_N and σ_i is the corresponding electron heavy-particle cross section. Inserting (1) into the RHS of (3) gives

$$\hat{J}(f) \equiv \hat{J}_i + \hat{J}_N = \int[f'(1-\xi f)F_{01}' - f(1-\xi f')F_{01}]\sigma g d\Omega dv_1 \tag{5}$$

Here σ represents the composite cross section

$$\sigma = a_C\sigma_C + a_N\sigma_N \tag{6}$$

Combining (5) and (3) gives our starting kinetic equation for the subsequent analysis. We will apply this equation to an equilibrium homogeneous plasma for purposes of calculating electrical conductivity. There results

$$\frac{e\underset{\sim}{E}}{m} \cdot \frac{\partial f}{\partial \underset{\sim}{v}} = \hat{J}(f) \tag{7}$$

with $\hat{J}(f)$ given by (5).

Lorentz Expansion

To account for anisotropy in the distribution $f(\underset{\sim}{v})$ we expand it in Legendre polynomials as follows.

$$f(\underset{\sim}{v}) = \sum_{\ell=0}^{\infty} P_\ell(\mu) f_\ell(v) \tag{8}$$

where

$$\mu \equiv \hat{\underset{\sim}{v}} \cdot \hat{\underset{\sim}{E}} \tag{9}$$

and hatted variables are unit vectors. Substituting (8) into the LHS of (7) and keeping $\ell = 1$ terms gives

$$\hat{\underset{\sim}{E}} \cdot \frac{\partial f}{\partial \underset{\sim}{v}} = \frac{P_o}{3}\left(\frac{df_1}{dv} + \frac{2f_1}{v}\right) + P_1 \frac{df_o}{dv} \tag{10}$$

Substituting the series (8) into the RHS of (7) we obtain

$$\hat{J}(f_o + \mu f_1) = \hat{J}(f_o) + \Delta\hat{J}(f_o, f_1) \tag{11a}$$

where

$$\Delta\hat{J}(f_o,f_1) = \int\{[\mu' f_1'(1-\xi f_o-\xi\mu f_1) - f_o'(\xi\mu f_1)]F_{01}' - [\mu f_1(1-\xi f_o'-\xi\mu' f_1') - f_o(\xi\mu' f_1')]F_{01}\}\sigma g d\Omega d\underset{\sim}{v}_1 \tag{11b}$$

[Note that $f_1 = f_1(v)$ whereas $F_{01} = F_0(v_1)$.] With

$$\varepsilon^2 \equiv \frac{m}{m+M}$$

taken as a parameter of smallness we find (see appendix A)

$$F_{01}' = F_{01} + O(\varepsilon) ,$$

$$v' = v + O(\varepsilon)$$

Keeping terms of leading order, (11b) becomes

$$\Delta\hat{J}(f_o,f_1) \equiv n_o f_1 \int (\mu'-\mu)\sigma g d\Omega \tag{12}$$

With

$$Q(v) \equiv \int(1-\cos\theta)\,\sigma(v,\theta)d\Omega \tag{13}$$

the preceding equation becomes, to this same order (see Appendix B)

$$\Delta\hat{J}(f_o, f_1) = -n_o f_1 \mu v Q \tag{14}$$

Combining (7, 10, 11 and 14) and equating coefficients of like Legendre-polynomial degree gives

$$\frac{eE}{3m}\left(\frac{df_1}{dv} + \frac{2f_1}{v}\right) = J(f_o) \tag{15a}$$

$$\frac{eE}{m}\frac{df_o}{dv} = -n_o f_1 v Q \tag{15b}$$

We note that (15a) may be rewritten

$$\frac{eE}{3m}\frac{1}{v^2}\frac{d}{dv}(v^2 f_1) = J(f_o) \tag{16}$$

Integrating $\underset{\sim}{v}$ in this equation over a sphere of radius $\tilde{v}$ we find

$$\frac{4\pi eE}{3m}\tilde{v}^2 f_1(\tilde{v}) = I(\tilde{v}) \tag{17}$$

where

$$I(\tilde{v}) \equiv \int\{\int_o^{\tilde{v}} [f_o'(1-\xi f_o)F_{01}' - f_o(1-\xi f_o')F_{01}]\sigma g v^2 dv\} d\Omega d\Omega_v d\underset{\sim}{v}_1 \tag{18}$$

and

$$d\underset{\sim}{v} = v^2 dv d\Omega_v$$

Evaluation of $I(\tilde{v})$

As is shown in Appendix C, $I(\tilde{v})$ may be reduced to the form (to leading order in ε)

$$I(\tilde{v}) = \int\left[\int_{\tilde{v}}^{\tilde{v}+\Delta v} f_o(1-\xi f_o')F_{01}\sigma g v^2 dv\right] d\Omega d\Omega_v d\underset{\sim}{v}_1 \tag{19}$$

where

$$\Delta v = \underset{\sim}{v}_1 \cdot (\hat{\underset{\sim}{g}} - \hat{\underset{\sim}{g}}') \tag{20}$$

We concentrate on the integrand of (19)

$$X \equiv f_o(1-\xi f_o')F_{01}\sigma g v^2 \tag{21}$$

With the observations

$$\tilde{v} < v < \tilde{v} + \Delta v, \qquad \Delta v = O(\varepsilon)$$

we expand

$$f_o = f_o(v) = f_o(\tilde{v}) + (v-\tilde{v})\frac{df_o(\tilde{v})}{dv} + \ldots$$

$$f_o' = f_o(v') = f_o(\tilde{v}) + (v'-\tilde{v})\frac{df_o(\tilde{v})}{dv} + \ldots$$

and obtain, to leading order in ε,

$$X = \Psi_1 f_o(\tilde{v})[1-\xi f_o(\tilde{v})] + \Psi_2\frac{df_o(\tilde{v})}{dv} + \Psi_3\xi f_o(\tilde{v})\frac{df_o(\tilde{v})}{dv} \tag{22}$$

where $\Psi_i(\underset{\sim}{v},\tilde{v},\theta,\underset{\sim}{v}_1)$ are known functions (see Appendix D.)

Writing (18) to leading order in ε we find

$$I = I_1 f_o(1-\xi f_o) + I_2\frac{df_o}{dv} + I_3\xi f_o\frac{df_o}{dv} \tag{23}$$

where

$$I_j \equiv \iint_{\tilde{v}}^{\tilde{v}+\Delta v} \psi_j dv d\Omega_v d\Omega d\underset{\sim}{v}_1 \tag{24}$$

Following a technique introduced by Davydov[11] we concentrate on I_2.

$$I_2 = \iint_{\tilde{v}}^{\tilde{v}+\Delta v} (v-\tilde{v}) F_{01}(v_1)\sigma(\tilde{v},\theta)\tilde{v}^3 dv d\Omega_v d\Omega d\underset{\sim}{v}_1 \tag{25}$$

Integrating over v and noting the equality

$$\int \hat{\underset{\sim}{v}}_1 \hat{\underset{\sim}{v}}_1 d\underset{\sim}{v}_1 = \frac{\bar{\bar{I}}}{3} \int d\underset{\sim}{v}_1$$

(where $\bar{\bar{I}}$ is the unit tensor) we find

$$I_2 = \frac{1}{3} \int v_1^2 (1-\cos\theta) F_{01}(v_1)\sigma(\tilde{v},\theta)\tilde{v}^3 d\Omega_v d\Omega d\underset{\sim}{v}_1$$

With the distribution (2) we note that

$$\int F_{01}(v_1) \frac{1}{2} M v_1^2 d\underset{\sim}{v}_1 = \frac{3}{2} n_o k_B T$$

which gives

$$I_2 = 4\pi\tilde{v}^3 \frac{n_o k_B T}{M} Q(\tilde{v}) \tag{26}$$

It is evident from (18) that $I(\tilde{v})$ depends on E only through its dependence on f_o. However we see that I_j as given by (23,24) do not depend on f_o. With this observation we evaluate I_j from 17) by setting $E = 0$. We choose $f_o(v,E)$ at $E = 0$ to be the Fermi Dirac distribution

$$f_o(v,o) = \frac{1}{\xi + \bar{B}_o \exp(mv^2/2k_B T)} \tag{27}$$

which has the properties

$$\frac{df_o(v,0)}{dv} = -\frac{mv}{k_B T}(1-\xi f_o)f_o \tag{28}$$

Furthermore, $f_o(v,E)$ is normalized by

$$\int_0^\infty f_o\, 4\pi v^2 dv = n \tag{29}$$

where n is electron density. With this distribution at hand we obtain

$$I_1 = \frac{m\tilde{v}}{k_B T} I_2 , \qquad I_3 = 0 \tag{30}$$

Inserting these values into (23) gives the result

$$I(\tilde{v}) = \frac{4\pi n_o \tilde{v}^3 Q(\tilde{v})}{M}\left[m\tilde{v} f_o(\tilde{v})(1-\xi f_o(\tilde{v})) + k_B T \frac{df_o}{d\tilde{v}}(\tilde{v})\right] \tag{31}$$

With $I(\hat{v})$ thus evaluated we return to (17).

<u>Equation for $f(\underset{\sim}{v})$</u>

Combining (15b) and (17) gives

$$-\frac{4\pi}{3}\left(\frac{eE}{m}\right)^2 \frac{\tilde{v}}{n_o Q}\frac{df_o}{dv} = I(\tilde{v}) \tag{32}$$

Inserting (31) into this equation and introducing the dimensionless energy,

$$x \equiv \frac{mv^2}{2k_B T} \tag{33}$$

gives, after some reduction, the nonlinear equation

$$[x+s(x)]\,\frac{df_o}{dx} + xf_o(1-\xi f_o) = 0 \tag{34}$$

where

$$s \equiv \frac{1}{6}\,\frac{M}{m}\left(\frac{eE}{n_o Q k_B T}\right)^2 \tag{35}$$

Integrating (34) we find

$$f_o(x) = \frac{1}{\xi + \overline{B}e^{A(x)}} \tag{36}$$

where

$$A(x) \equiv \int_0^x \frac{x'dx'}{x' + s(x')} \tag{37}$$

First note that (36) and (37) give

$$\frac{df_o}{dx} = -\frac{x}{x+s}\,(1-\xi f_o)f_o \tag{38}$$

which is seen to reduce to (28) in the limit $s = 0$.

With (38) and recalling (8) and (15b), we obtain the total distribution function

$$f(x) = f_o(x)\{1-u[6\varepsilon s(x)]^{1/2}\,\frac{x}{x+s(x)}\,[1-\xi f_o(x)]\} \tag{39}$$

It is convenient at this point to introduce the dimensionless distribution[18]

$$\overline{f}_{SL}(x) = \xi f_o(x) = \frac{1}{1 + Be^{A(x)}} \tag{40}$$

where $B \equiv \overline{B}/\xi$. This distribution has the normalization

$$\int_0^\infty \bar{f}_{SL}(x)x^{1/2}dx = \frac{\sqrt{\pi}}{2}\Lambda_Q \tag{41}$$

where

$$\Lambda_Q \equiv n\,\lambda_d^3 \tag{42a}$$

and λ_d is the thermal deBroglie wavelength

$$\lambda_d^2 = \frac{2\pi\hbar^2}{mk_BT} \tag{42b}$$

Note that in the classical limit,[14] $\xi \to 0$ [see (4b)] and $f_{SL}(x)$ goes to the Druyvesteyn distribution.[10] For low electric field, from (35,37) we see that $s \approx 0$, $A(x) \approx x$ and (38,39) return the displaced Fermi-Dirac distribution.[19]

Conductivity

Calculation of Q integrals

Employing the distribution (39) gives the current density (after an integration by parts)

$$\underset{\sim}{J} = \frac{8\pi}{3}\,\underset{\sim}{E}\left(\frac{e}{m}\right)^2 \frac{k_BT}{n_o}\int_0^\infty \frac{d}{dx}\left(\frac{x}{Q}\right)\bar{f}_{SL}(x)dx \tag{43}$$

Evaluation of the integral in this expression demands knowledge of $Q(x)$ as given by (13). Inserting the composite cross section (6) into (13) we find

$$Q = \int(1-\cos\theta)[a_C\sigma_C + a_N\sigma_N]d\Omega \tag{44a}$$

or, equivalently,

$$Q = Q_C + Q_N \tag{44b}$$

where Q_C and Q_N correspond to the charge and neutral components of (44a), respectively. For Q_C we employ the results of Liboff[20] for the high-energy domain and those of Chapman and Cowling[15] relevant to the low-energy domain. In the first of these calculations the electron-ion interaction potential was taken to be

$$V(r) = \frac{Ze^2}{r} \exp(-r/\lambda_D) \tag{45a}$$

where the Debye distance λ_D is given by

$$\lambda_D^{-2} = \frac{4\pi a_C n_o e^2}{k_B T} Z(Z+1) \tag{45b}$$

In the low-energy calculation the potential was taken to be

$$V(r) = \frac{Ze^2}{r}, \qquad r < \lambda_D \tag{46}$$

and zero for $r \geq \lambda_D$. Related cross sections are as follows. We introduce the dimensionless cross section

$$Q \equiv \pi \Delta^2 \tilde{Q} \tag{47}$$

where

$$\Delta \equiv \frac{Ze^2}{k_B T}$$

is the so-called "distance of closest approach." Liboff's result may then be written

$$\tilde{Q}_{C,L} = \frac{a_C}{x^2} \left[\ln \frac{2x}{\Gamma_D} + \beta \right] \tag{48}$$

$$\beta \equiv \ln 2 - \gamma - \frac{1}{2}$$

where γ is Euler's constant and

$$\Gamma_D \equiv \frac{\Delta}{\lambda_D}$$

is the conventional plasma parameter. Chapman-Cowling's result appears as

$$\tilde{Q}_{C,C-C} = \frac{a_C}{2x^2} \ln\left[1 + \left(\frac{2x}{\Gamma_D}\right)^2\right] \tag{49}$$

A smooth interpolation formula bridging the two results (48,49) is given by

$$\tilde{Q}_C = \frac{a_C}{x^2}\left\{\frac{1}{2} \ln\left[1 + \left(\frac{2x}{\Gamma_D}\right)^2\right] + \beta\left[1 - \exp\left(-\frac{x^4}{\Gamma_D^4}\right)\right]\right\} \tag{50}$$

See Fig. 1. For $x \gtrsim \Gamma_D$, (50) gives $\tilde{Q}_C \approx \tilde{Q}_{C,L}$ whereas for $x \lesssim \Gamma_D$, it gives $\tilde{Q}_C \approx \tilde{Q}_{C,C-C}$.

Lastly for Q_N we set[21]

$$\sigma_N = \frac{(\alpha a_o)^2}{4} \tag{51}$$

where α is a pure number between one and six and a_o is the Bohr radius. For example, for Al, $\alpha \approx 2.4$. With (51) we find

$$\tilde{Q}_N = a_N \left(\frac{\alpha a_o}{\Delta}\right)^2 \tag{52}$$

Substituting (50) and (52) into (44b) gives the desired composite $\tilde{Q}$.

With (47), the expression (35) may be rewritten

$$s = \left(\frac{E}{E_o}\right)^2 \tilde{Q}^{-2} \tag{53}$$

where the characteristic electric field

$$E_o = \sqrt{\frac{6m}{M}} \; \frac{n_o \pi \Delta^2 k_B T}{e} \tag{54}$$

Furthermore we note that the parameters Γ_D and Λ_Q may be conveniently written in terms of the Bohr radius, $a_o \equiv \hbar^2/me^2$ and Rydberg, $R \equiv e^2/2a_o$.

$$\Gamma_D^2 = 4\pi a_C Z^3 (Z+1)(n_o a_o^3)\left(\frac{2R}{k_B T}\right)^3 \tag{55a}$$

$$\Lambda_Q^2 = (2\pi)^3 a_C^2 Z^2 \left(n_o a_o^3\right)^2 \left(\frac{2R}{k_B T}\right)^3 \tag{55b}$$

These forms give

$$n_o a_o^3 = \frac{Z(Z+1)}{2\pi^2 a_C} \frac{\Lambda_Q^2}{\Gamma_D^2} \tag{56a}$$

$$\left(\frac{k_B T}{2R}\right)^3 = \frac{2}{\pi} Z^4 (Z+1)^2 \frac{\Lambda_Q^2}{\Gamma_D^4} \tag{56b}$$

with these expressions at hand E_o as given by (54) may be written

$$\frac{E_o}{e/a_o^2} = \frac{3^{1/2}}{2^{5/6}\pi^{2/3}} \left(\frac{m}{M}\right)^{1/2} \frac{Z^{5/3}(Z+1)^{1/3}}{a_C} \frac{\Lambda_Q^{4/3}}{\Gamma_D^{2/3}} \tag{57}$$

where $e/a_o^2 = 5.14 \times 10^9$ V/cm.

Evaluation of Conductivity

Rewriting (43) in the form

$$\underset{\sim}{J} = \sigma \underset{\sim}{E} \tag{58}$$

and setting

$$\tilde{\sigma} = \sigma/\omega_p \tag{59}$$

where

$$\omega_p^2 = \frac{4\pi a_C n_o Z e^2}{m}$$

we obtain

$$\tilde{\sigma} = \frac{1}{3}\left(\frac{2}{\pi}\right)^{3/2} \frac{a_C(Z+1)^{1/2}}{\Lambda_Q \Gamma_D} \int_0^\infty \bar{f}_{SL}(x) \frac{d}{dx}\left(\frac{x}{\tilde{Q}}\right) dx \tag{60}$$

where $\bar{f}_{SL}(x)$ is given by (40) and $\tilde{Q}$ by (46b), (50) and (52). Note that $\tilde{\sigma}$ as given by (60) is a function of E, Z, a_C, n_o and T where, we recall, T is heavy-particle temperature. We apply this formula to an aluminum plasma with $n_o = 10^{20}$ and $k_B T = 5$eV for which $Z \simeq 2.5$. With these values, (57) gives $E_o = 8.97 \times 10^4$ V/cm. Taking $\alpha = 2.4$ in (51) permits evaluation of $\tilde{\sigma}$ as given by (60) with a_C a free variable. Numerical plots of $\tilde{\sigma}$ vs (E/E_o) for these values at $a_C = 0.1$, 0.5 and 0.9 are shown in Fig. 2.

Three regions of behavior are apparent from these curves. For low electric field the curves are seen to obey Ohm's law. At $E \approx 0.1E_o$ nonlinear effects due to the Coulomb cross section come into play which are evidently more pronounced for higher ion density, $a_C n_o$. At $E \approx 0.3E_o$ the Coulomb cross section gives way to the cross section of the neutrals resulting in a $E^{-1/2}$ fall off of conductivity.

Conclusions

Starting with the Uehling-Uhlenbeck quasi-classical kinetic equation we have addressed the problem of nonlinear electrical conductivity in a plasma comprised of electrons, ions and neutrals. A Legendre polynomial expansion was introduced to account for anisotropy of the electron distribution function due to the applied electric field. An interpolation was introduced to bridge the low and high energy components of the electron-ion cross section. An exact solution of the resulting equation for the electron distribution was obtained which was found to go to consistent limits in the classical and quantum limits. With this distribution at hand an explicit formula for electrical conductivity was obtained in terms of E, Z, a_C, n_o and T. Numerical plots of conductivity vs electric field for a specific case of an aluminum plasma at varying values of a_C were obtained. These curves revealed three distinct domains of behavior which were associated with various components of the cross section.

Appendix A

In this appendix we wish to justify the relations preceding (12). With

$$\varepsilon^2 \equiv \frac{m}{M+m} \tag{A1}$$

the center of mass velocity is given by

$$\underset{\sim}{G} = \varepsilon^2 \underset{\sim}{v} + (1-\varepsilon^2)\underset{\sim}{v}_1 \tag{A2}$$

With relative velocities defined by

$$\underset{\sim}{g} = \underset{\sim}{v} - \underset{\sim}{v}_1 \tag{A3.a}$$

$$\underset{\sim}{g}' = \underset{\sim}{v}' - \underset{\sim}{v}_1' \tag{A3.b}$$

we find

$$v'^2 = v^2 + 2(1-\varepsilon^2)\underset{\sim}{G} \cdot (\underset{\sim}{g}' - \underset{\sim}{g}) \tag{A4.a}$$

$$v_1'^2 = v_1^2 - 2\varepsilon^2 \underset{\sim}{G} \cdot (\underset{\sim}{g}' - \underset{\sim}{g}) \tag{A4.b}$$

Dropping terms of order ε^2 then gives

$$v' = v + \frac{\underset{\sim}{v}_1 \cdot (\underset{\sim}{g}' - \underset{\sim}{g})}{v} \tag{A5.a}$$

$$v_1' = v_1 \tag{A5.b}$$

The latter of these relations gives, to $O(\varepsilon^2)$, the desired result

$$F_{01}' = F_{01}$$

For electron temperature T_e equal to or in excess of ion temperature T, we write

$$\frac{3}{2} k_B T = \langle \frac{1}{2} Mv^2 \rangle \lesssim \langle \frac{1}{2} mv^2 \rangle = \frac{3}{2} k_B T_e \tag{A6}$$

or equivalently, $\langle x \rangle \gtrsim 1$. In addition this relation gives

$$\frac{v_1}{v} \sim \varepsilon \tag{A7}$$

This result together with (A3.a) permits (A5.a) to be written

$$v' = v + \underset{\sim}{v}_1 \cdot (\hat{\underset{\sim}{g}}' - \hat{\underset{\sim}{g}}) \tag{A8}$$

which to $O(\varepsilon)$ returns the relation

$$v' = v \tag{A9}$$

Appendix B

We wish to derive (14). Recalling (12) we write

$$\Delta\hat{J}(f_o,f_1) = n_o f_1 \int (\mu' - \mu)\sigma g d\Omega \tag{B1}$$

Dropping terms of order ε, we note

$$\mu \equiv \hat{\underset{\sim}{v}} \cdot \hat{\underset{\sim}{E}} = \hat{\underset{\sim}{g}} \cdot \hat{\underset{\sim}{E}}$$

$$\mu' \equiv \hat{\underset{\sim}{v}}' \cdot \hat{\underset{\sim}{E}} = \hat{\underset{\sim}{g}}' \cdot \hat{\underset{\sim}{E}} \tag{B2}$$

$$g = v$$

With $\underset{\sim}{g} = g(0,0,1)$, $\underset{\sim}{E} = E(\sin\alpha,\ 0,\ \cos\alpha)$ and $g' = g(\sin\theta\cos\phi,\ \sin\theta\sin\phi,\ \cos\theta)$

$$\mu' = \cos\alpha\cos\theta + \sin\alpha\sin\theta\cos\phi \tag{B3}$$

$$\mu = \cos\alpha$$

Integration over $d\Omega$ gives no contribution from the $\cos\phi$ term of μ'. There results

$$\Delta\hat{J}(f_o,f_1) = -\, n_o f_1 v\mu \int (1-\cos\theta)\sigma d\Omega \tag{B4}$$

which with (13) returns (14).

Appendix C

In this appendix, we wish to derive (19). Recalling (18) we write

$$I(\tilde{v}) \equiv \int \left\{ \int_0^{\tilde{v}} [f_o'(1-\xi f_o)F_{01}' - f_o(1-\xi f_o')F_{01}]\sigma g v^2 dv \right\} d\Omega d\Omega_v d\underset{\sim}{v}_1 \qquad \text{(C1)}$$

Consider the transformation which exchanges primed with unprimed variables. We find

$$g \equiv |\underset{\sim}{v}-\underset{\sim}{v}_1| = |\underset{\sim}{v}'-\underset{\sim}{v}_1'| \equiv g' \qquad \text{(C2a)}$$

$$d\underset{\sim}{g}\, d\underset{\sim}{v}'\, d\underset{\sim}{v}_1' = d\underset{\sim}{g}'\, d\underset{\sim}{v}\, d\underset{\sim}{v}_1 \qquad \text{(C2b)}$$

$$\sigma(\underset{\sim}{g}) = \sigma(\underset{\sim}{g}') \qquad \text{(C2c)}$$

where (C2c) holds due to the invariance of the inverse cross-section.[17] With (C2) at hand, we obtain

$$\iint_{|\underset{\sim}{v}|<\tilde{v}} f_o'(1-\xi f_o)F_{01}'\sigma g d\underset{\sim}{v} d\Omega d\underset{\sim}{v}_1 = \iint_{|\underset{\sim}{v}'|<\tilde{v}} f_o(1-\xi f_o)F_{01}\sigma g d\underset{\sim}{v} d\Omega d\underset{\sim}{v}_1 \qquad \text{(C3)}$$

From (A8) $|\underset{\sim}{v}'| < \tilde{v}$ and $|\underset{\sim}{v}| < \tilde{v} + \underset{\sim}{v}_1 \cdot (\hat{\underset{\sim}{g}} - \hat{\underset{\sim}{g}}')$ are equivalent to order ε. Combining this fact with (C1) and (C3) returns the desired result, (19).

Appendix D

In this appendix the functions Ψ_i of (22) are found. With the observations

$$\tilde{v} < v < \tilde{v} + \Delta v \tag{D1}$$

and that Δv as given by (20) is of order ε, we find

$$g = \tilde{v} + O(\varepsilon) \tag{D2a}$$

$$v^2 = \tilde{v}^2 + O(\varepsilon) \tag{D2b}$$

$$v - \tilde{v} = O(\varepsilon) \tag{D2c}$$

$$v' - \tilde{v} = O(\varepsilon) \tag{D2d}$$

$$\sigma(g,\hat{\underset{\sim}{g}}') = \sigma(\tilde{v},\hat{\underset{\sim}{g}}') + O(\varepsilon) \tag{D2e}$$

Inserting these expressions into (21) and expanding f_o and f_o' about $\tilde{v}$, we obtain

$$\begin{aligned} X \equiv f_o(1-\xi f_o')F_{01}\sigma g v^2 &= f_o(\tilde{v})(1-\xi f_o(\tilde{v}))F_{01}(v_1)\sigma(\tilde{v},\hat{g}')\tilde{v}^3 \\ &+ (v-\tilde{v})\frac{df_o}{dv}(\tilde{v})(1-\xi f_o(\tilde{v}))F_{01}(v_1)\sigma(\tilde{v},\hat{g}')\tilde{v}^3 \\ &- \xi f_o(\tilde{v})(v'-\tilde{v})\frac{df_o}{dv}(\tilde{v})F_{01}(\tilde{v}_1)\sigma(\tilde{v},\hat{\underset{\sim}{g}}')\tilde{v}^3 \\ &+ A(\hat{\underset{\sim}{g}}',\tilde{v},\hat{\underset{\sim}{v}},\underset{\sim}{v}_1)f_o(\tilde{v})(1-\xi f_o(\hat{v}))F_o(v_1) + O(\varepsilon^2) \end{aligned} \tag{D3}$$

where the function $A(\hat{\underset{\sim}{g}}',\tilde{v},\hat{\underset{\sim}{v}},\underset{\sim}{v}_1)$ is of order ε. Comparison of the above expression with (22) serves to identify the Ψ_i functions.

References

1. R. Kubo, in Lectures in Theoretical Physics, edited by W. E. Brittin and L. G. Dunham (Interscience, New York, 1959), Vol. 1.

2. D. B. Boercker, Phys. Rev. A 23, 1969 (1981).

3. R. H. Williams and H. E. DeWitt, Phys. Fluids 12, 2326 (1969).

4. M. Lampe, Phys. Rev. 170, 306 (1968).

5. Y. T. Lee and R. M. More, Phys. Fluids 27, 1273 (1984).

6. E. Gross, D. Bhatnager, and M. Krook, Phys. Rev. 94, 511 (1954).

7. H. Dreicer, Phys. Rev. 117, 343 (1960).

8. E. A. Uehling and G. E. Uhlenbeck, Phys. Rev. 43, 552 (1933).

9. H. A. Lorentz, The Theory of Electrons (B. G. Teubner, Leipzig, 1909, and G. E. Stechert and Company, New York, 1923).

10. M. J. Druyvesteyn, Physica 10, 61 (1930).

11. B. Davydov, Phys. Z. Sowj. Un. 8, 59 (1935).

12. W. P. Allis, Hand. d. Physik (Springer-Verlag, Berlin, 1955).

13. H. Dreicer, Phys. Rev. 115, 238 (1959).

14. R. L. Liboff, J. Appl. Phys. 56, 2530 (1984).

15. S. Chapman and T. G. Cowling, The Mathematical Theory of Non-Uniform Gases, 3rd. ed., (Cambridge, London, 1970).

16. R. L. Liboff and G. K. Schenter, "Solution to a new non-linear equation for the transport of charge carriers in a semiconductor." Submitted for publication to Phys. Rev. B. Feb. (1986)

17. R. L. Liboff, Introduction to the Theory of Kinetic Equations, (Krieger Press, Melbourne, FL 1979).

18. The distribution (40) was obtained previously for the case s (and therefore Q) equal to a constant and was labeled f_{SL} (as opposed to $\bar{f}_{SL}$ of the present work). See reference 16.

19. C. Kittel, Introduction to Solid State Physics, 3rd ed. (Wiley, New York, 1968).

20. R. L. Liboff, Phys. Fluids 2, 40 (1959).

21. D. D. Clark, personal communication.

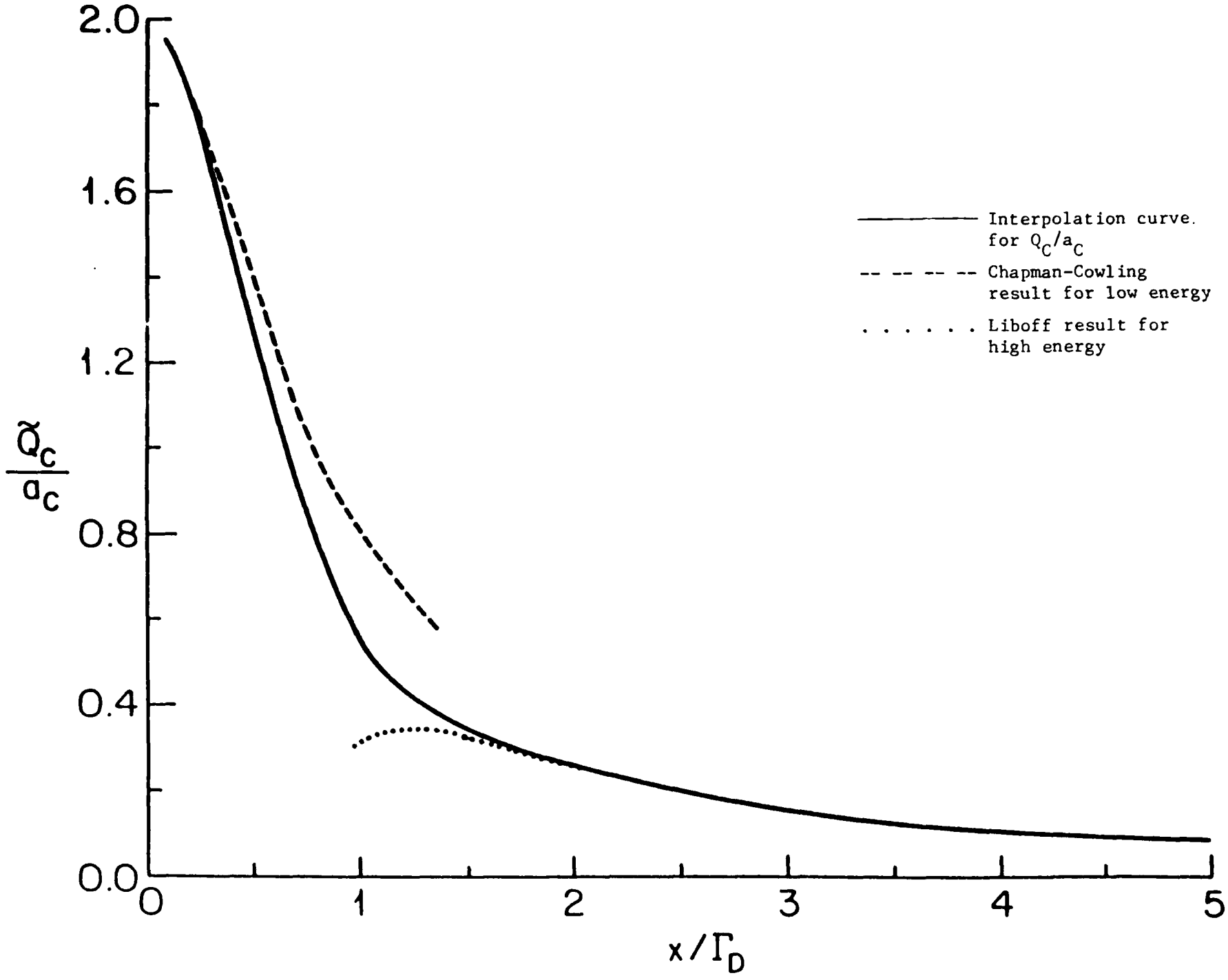
2.0
1.6
1.2
0.8
0.4
0.0
$\frac{Q_C}{a_C}$
0
1
2
3
4
5
x/Γ_D
Interpolation curve for Q_C/a_C
Chapman-Cowling result for low energy
Liboff result for high energy

Figure 1

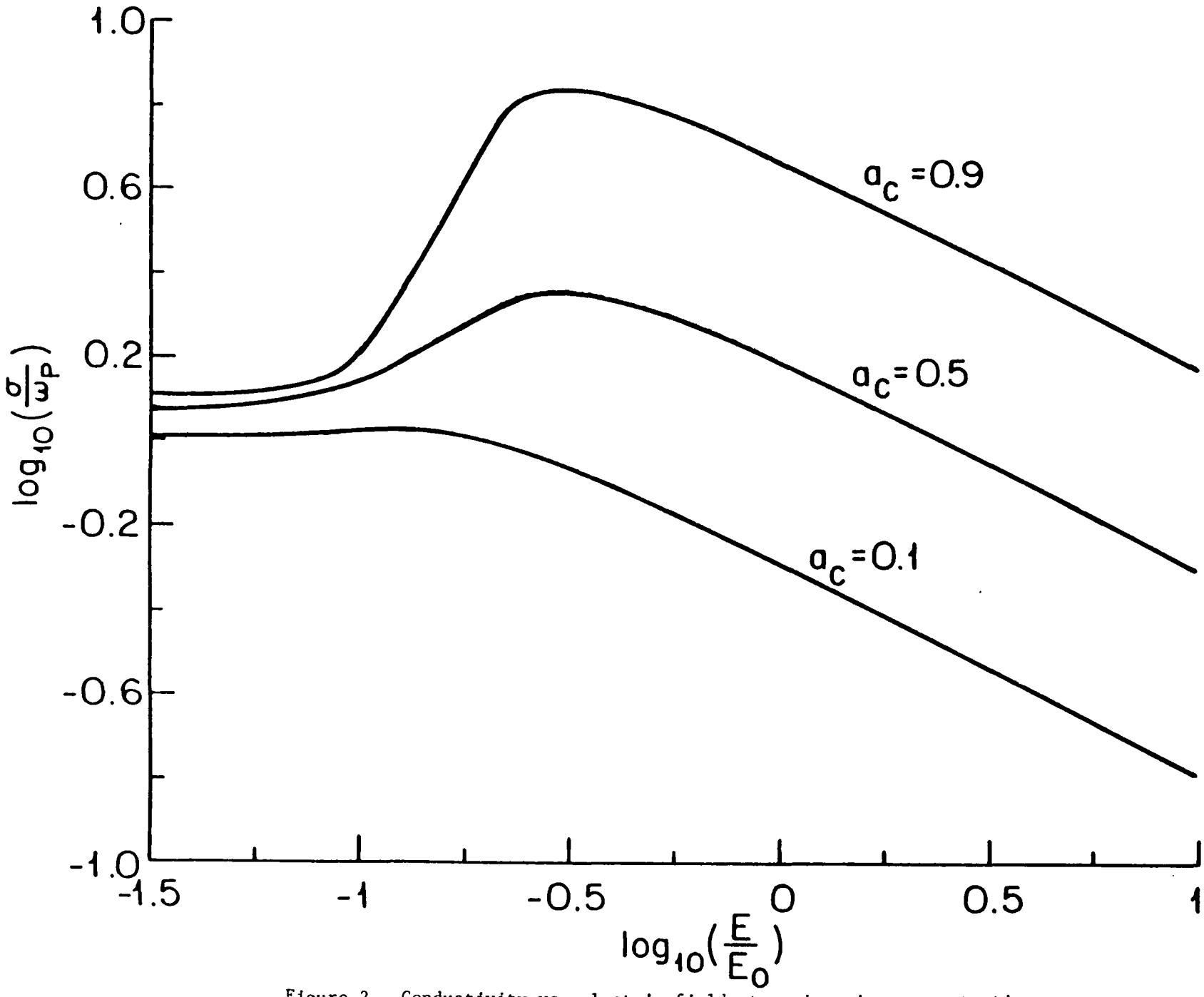

Figure 2. Conductivity vs. electric field at various ion concentrations

Acknowledgments

The author wishes to express deep appreciation to his colleague, Gregory K. Schenter, for invaluable assistance rendered in the preparation of this report.

DISTRIBUTION LIST

Commander
Armament Research, Development and
Engineering Center
ATTN: SMCAR-MSI (5)
SMCAR-FSA-E (12)
SMCAR-SF
Dover, NJ 07801-5001

Commander
U.S. Army Armament, Munitions and
Chemical Command
ATTN: AMSMC-GCL(D)
Dover, NJ 07801-5001

Administrator
Defense Technical Information Center
ATTN: Accessions Division (2)
Cameron Station
Alexandria, VA 22304-6145

Director
U.S. Army Materiel Systems Analysis Activity
ATTN: AMXSY-MP
Aberdeen Proving Ground, MD 21005-5066

Commander
Chemical Research and Development Center
U.S. Army Armament, Munitions and
Chemical Command
ATTN: SMCCR-SPS-IL
Aberdeen Proving Ground, MD 21010-5432

Commander
Chemical Research and Development Center
U.S. Army Armament, Munitions and
Chemical Command
ATTN: SMCCR-RSP-A
Aberdeen Proving Ground, MD 21010-5432

Director
Ballistic Research Laboratory
ATTN: AMXBR-OD-ST
Aberdeen Proving Ground, MD 21005-5066

Chief
Benet Weapons Laboratory, CCAC
Armament Research, Development and
Engineering Center
U.S. Army Armament, Munitions and Chemical Command
ATTN: SMCAR-CCB-TL
Watervliet, NY 12189-5000

Commander
U.S. Army Armament, Munitions and
Chemical Command
ATTN: SMCAR-ESP-L
Rock Island, IL 61299-6000

Commander
U.S. Army Armament, Munitions
and Chemical Command
ATTN: AMSMC-QAR-R(D)
Dover, NJ 07801-5001

Director
U.S. Army TRADOC Systems
Analysis Activity
ATTN: ATAA-SL
White Sands Missile Range, NM 88002

Director
Defense Advanced Research Projects Agency
ATTN: DARPA-TTO, H.D. Fair, Jr. (5)
1400 Wilson Boulevard
Arlington, VA 22209

Commander
U.S. Army Strategic Defense Command
ATTN: DASD-DP, LTC N. Cooney (2)
P.O. Box 15280
Arlington, VA 22215-0151

System Planning Corporation
ATTN: Donald E. Shaw
1500 Wilson Boulevard
Arlington, VA 22209-2454

Center for Electromechanics
ATTN: W. Weldon (2)
10100 Burnet Road
Austin, TX 78758

Commander
HQ, AFSC/DLWA
ATTN: R. Reynolds
Andrews Air Force Base, MD 20334

Commander
Naval Sea Systems Command
ATTN: LCDR Joseph R. Costa
Washington, DC 20362

Commander
Air Force Armament Technology Laboratory
ATTN: DLDG, Timothy Aden
Eglin Air Force Base, FL 32542-5270

Commander
U.S. Army Research Office
ATTN: AMXRO-PR, H.T. Throckmorton
P.O. Box 12211
Research Triangle Park, NC 27709

Commander
Strategic Defense Initiative Organization
ATTN: SDIO/KEW, BG M. O'Neill (2)
Washington, DC 20301-7100

Electromagnetic Launch Research, Inc.
ATTN: Henry Kolm
Peter P. Mongeau
625 Putnam Avenue
Cambridge, MA 92139

Westinghouse Electric Company
ATTN: Lan R. McNab, Manager
EML Engineering
Marine Division, MS ED-5
401 E. Hendy Avenue
P.O. Box 499
Sunnyvale, CA 94088

Brookhaven National Laboratory
ATTN: James P. Powell, Jr.,
Head, Fusion Technology Group
Building 820M
Upton, NY 11973

General Electric Company
ATTN: Alan Wait, Manager
EML Systems Technology
RD-3 Plains Road
Ballston Spa, NY 12020

END

1-87

DTIC